



PU/PET Scaffold Utilized for a Stem Cell-Based Atrioventricular Nodal Bypass Device

A Major Qualifying Project Report:
Submitted to the Faculty
Of the
WORCESTER POLYTECHNIC INSTITUTE
In Partial Fulfillment of the Requirements For the
Degree of Bachelor of Science
By

Katherine Connors

Rachel Feyler

Vanessa Gorton

Katelyn Nicosia

Date: April 30, 2015

Submitted to:

Professor Glenn Gaudette, Advisor

Table of Contents

Table of Figures	5
Table of Tables	7
Authorship Page.....	8
Acknowledgements.....	10
Abstract.....	11
Chapter 1: Introduction.....	12
Chapter 2: Literature Review.....	14
2.1 Structure and Mechanical System of the Heart.....	14
2.2 Electrical System of the Heart	16
2.3 Electrical Propagation through the Heart.....	18
2.4 Heart Malfunctions: Arrhythmias and AV Nodal Block	21
2.5 Electronic Cardiac Pacemakers.....	24
2.6 Autonomic Response	25
2.7 Potential Cell Types.....	26
2.8 Fibrin Microthreads	28
2.9 Hollow Tubule Fibers	30
2.10 Electrospinning.....	32
2.11 BioGlue®.....	34
2.12 Heat Sealing.....	34
2.13 Cardiac Catheter.....	35
Chapter 3: Project Strategy.....	38
3.1 Initial Client Statement.....	38
3.2 Objectives	38
3.3 Functions and Specifications	46
3.4 Constraints	49
3.5 Revised Client Statement.....	50
3.6 Further Project Approach.....	50
Chapter 4: Alternative Designs.....	51
4.1 Conceptual Designs.....	51
4.1.1 Primary Conceptual Designs.....	52
4.1.2 Secondary Conceptual Designs.....	53

4.1.3	Final Conceptual Designs	54
4.2	Preliminary Designs	55
4.2.1	‘Flattened Straw’ Designs.....	56
4.2.2	Cylindrical Designs.....	57
4.3	Scaffold Material Analysis.....	58
4.3.1	Polyurethane	59
4.3.2	Polyethylene Terephthalate.....	60
4.3.2	Polytetrafluoroethylene.....	61
4.3.3	‘Poly-X’	61
4.4	Feasibility Analysis.....	62
4.4.1	Delivery Feasibility.....	62
4.4.2	Structure.....	63
4.4.3	Fabrication Methods	64
4.4.4	Sealing Methods.....	67
4.4.5	HCN Transfected Cell Availability	68
4.5	Decisions on Designs	68
4.5.1	Option 1: ‘Poly-X’ and PU/PET Hollow Tubes	68
4.5.2	Option 2: ‘Poly-X’ Hollow Tube and PU/PET Electrospinning	69
4.5.3	Option 3: PU/PET Electrospinning.....	70
4.5.4	Design Specifications.....	70
4.5.5	Design Calculations	72
4.6	Feasibility Testing.....	73
4.6.1	Sealing and Thread Insertion Methods	73
4.6.2	Cell Viability.....	76
4.6.3	Migration.....	76
Chapter 5:	Design Verification Results	78
5.1	LIVE/DEAD Staining.....	78
5.3	Cell Migration.....	79
5.3	Heat Sealing.....	80
Chapter 6:	Discussion	83
6.1	LIVE/DEAD Staining Results	83
6.2	Migration Study Results	84

6.3 Heat Sealing Results	84
6.4 Limitations in Design Verification	85
6.5 Device Impacts.....	86
Chapter 7: Final Design and Validations	89
Chapter 8: Conclusions and Recommendations	93
8.1 Future Testing Recommendations	93
8.1.1 Current Flow	93
8.1.2 Mechanical Stability	94
8.1.3 Gap Junction Formation.....	94
8.1.4 Physiological Autonomic Responsiveness	95
8.1.5 Delivery Verification	95
8.1.5 Conclusions.....	96
References.....	97
Appendices.....	104
Appendix I: Objectives Tree.....	104
Appendix II: Pairwise Comparison Charts	105
Appendix III: LIVE/DEAD Staining Protocol	107
Appendix IV: Hoechst and Phalloidin Staining Protocol	108
Appendix V: Immunohistochemistry Cx43 Staining Protocol	109

Table of Figures

Figure 1: Heart location in relation to the rib cage and spinal column.....	14
Figure 2: Diagram of the four chambers and valves of the heart.....	15
Figure 3: Electrical conduction pathway of the heart.....	18
Figure 4: Phases of action potential generation displayed in a membrane potential versus time graph.....	20
Figure 5: Bradycardia and tachycardia displayed via an ECG.....	22
Figure 6: Image of the location of the electronic cardiac pacemaker.....	24
Figure 7: SEM image of polymeric fibers produced via electrospinning.....	32
Figure 8: Diagram of the electrospinning process.....	33
Figure 9: Bioglue Surgical Adhesive, CryoLife.....	34
Figure 10: J&L 60 Watts Soldering Iron.....	35
Figure 11: Delivery Mechanism of the Cardiac Catheter: Inner core and outer needle contained within the sheath.....	36
Figure 12: Insertion mechanism (read from left to right).....	37
Figure 13: First conceptual designs - funnel (left), socket (center) and bundle (right).....	53
Figure 14: Second conceptual designs: bundle (left), funnel (center) and socket (right).....	54
Figure 15: Final conceptual design in the form of the funnel scaffold.....	54
Figure 16: Key for the preliminary design images shown below.....	55
Figure 17: 'Flattened Straw' plain bundle (left) and 'Flattened Straw' funnel (right) preliminary designs.....	56
Figure 18: Cylinder plain bundle (left) and cylinder funnel preliminary designs.....	58
Figure 19: Design Option 1: Red is the PU/PET Hollow Tubes; Grey is the Poly-X Hollow Tube Scaffold.....	69
Figure 20: Design Option 2: Blue is the PU/PET Electropun Scaffolds; Grey is the 'Poly-X' Hollow Tube Scaffold.....	70
Figure 21: Design Option 3: Blue is the PU/PET Electrospun Scaffold.....	70
Figure 22: Thread Insertion Option 1.....	74
Figure 23: Thread Insertion Option 2.....	75
Figure 24: Thread Insertion Option 3.....	75
Figure 25: Gaudette-Pins Well.....	77
Figure 26: Samples 1 & 2: 20 μ m scaffolds with a 96.3% cell viability (left) and a 98.2% cell viability (right) with the scale bar representing 150 μ m.....	78
Figure 27: Samples 3 & 4: 40 μ m scaffolds with a 97.2% cell viability (left) and a 98.6% viability (right) with the scale bar representing 100 μ m.....	78
Figure 28: Hoescht and Phalloidin on top (left) and bottom (right) of 20 μ m scaffold with the scale bar representing 100 μ m.....	80
Figure 29: Hoechst and Phalloidin staining of top (left) and bottom (right) of the 40 μ m scaffold with the scale bar representing 100 μ m.....	80

Figure 30: Hoechst and Phalloidin staining on top (left) and bottom (right) of the 50 μm scaffold with the scale bars representing 100 μm	80
Figure 32: LIVE/DEAD staining of hMSCs on fibrin microthreads immediately after heat sealing 50 μm PU/PET scaffold.....	81
Figure 33: Final design with outer thick regions (blue), inner thin regions (pink) and a center thick region (blue) all at least 40-50 μm thick.....	89
Figure 34: Final design loaded onto specifically designed catheter	91
Figure 35: Assembly Method (left to right, top to bottom); a) hMSC seeded fibrin microthread suture is attached to a straight needle b) the suture is inserted and pulled through the cylindrical PU/PET scaffold c) the ends of the scaffold are clamped d) a fine-tip heat source is applied.	92

Table of Tables

Table 1: Results of PCCs comparing the team’s average with Professor Gaudette’s	39
Table 2: Results of Secondary PCCs comparing the team’s average with Professor Gaudette’s.	39
Table 3: Brainstorming activity results for the first three functions	51
Table 4: “Summary of Candidate Material Properties” [66]	62
Table 5: Ideal Design Specifications	71
Table 6: Results of LIVE/DEAD staining on four scaffold samples	79
Table 7: Cost of components needed in development of AV node bypass device	87

Authorship Page

	<u>Written By:</u>	<u>Edited By:</u>
Chapter 1: Introduction	VG	All
Chapter 2: Literature Review		
2.1 Structure and Mechanical System	KN	All
2.2 Electrical System	KN	All
2.3 Electrical Propagation	RF	All
2.4 Autonomic Response	KC	All
2.5 Heart Malfunctions	KC	All
2.6 Cardiac Electronic Pacemakers	VG	All
2.7 Potential Cell Types	RF	All
2.8 Fibrin Microthreads	KC	All
2.9 Hollow Tubule Fibers	KC	All
2.10 Electrospinning	KN	All
2.11 BioGlue	VG	All
2.12 Heat Sealing	VG	All
2.13 Cardiac Catheter	KC	All
Chapter 3: Project Strategy		
3.1 Initial Client Statement	KN	All
3.2 Objectives	RF	All
3.3 Constraints	VG	All
3.4 Functions and Specifications	KN	All
3.5 Revised Client Statement	KN	All
3.6 Further Project Approach	KN	All
Chapter 4: Alternative Designs		
4.1 Conceptual Designs	KN	All
4.1.1 Primary Conceptual Designs		
4.1.2 Secondary Conceptual Designs		
4.1.3 Final Conceptual Designs		
4.2 Preliminary Designs	KN	All
4.2.1 'Flattened Straw' Designs		
4.2.2 Cylindrical Designs		
4.3 Material Analysis	VG	All
4.3.1 Polyurethane		
4.3.2 Polyethylene Terephthalate		
4.3.3 Polytetrafluoroethylene		
4.3.4 'Poly-X'		
4.4 Feasibility Study	KC	All
4.4.1 Delivery Feasibility		

4.4.2 Mechanical Structure		
4.4.3 Fabrication Methods		
4.4.3.1 Laser Micro-etching		
4.4.3.2 Electrospinning		
4.4.3.3 Solvent Casting and Particulate Leaching		
4.4.3.3.1 Material Analysis		
4.4.3.3.2 Pore Size Analysis		
4.4.4 Sealing Methods		
4.4.4.1 Heat Sealing		
4.4.4.2 BioGlue		
4.4.5 HCN Transfected Cell Availability		
4.5 Decisions on Final Design	KN	All
4.5.1 Option 1: ‘Poly-X’ and PU/PET Hollow Tubes		
4.5.2 Option 2: ‘Poly-X’ Hollow Tube and PU/PET Electrospinning		
4.5.3 Option 3: PU/PET Electrospinning		
4.5.4 Design Specifications		
4.5.5 Design Calculation		
4.5.5.1 Surface Area of Cylindrical Bridge		
4.5.5.2 Forces Exerted by the Heart		
4.6 Feasibility Testing		
4.6.1 Sealing and Thread Insertion Methods	KN	All
4.6.2 Cell Viability	RF	All
4.6.3 Migration	RF	All
4.6.4 Gap Junction Formation	RF	All
Chapter 5: Design Verification	RF	All
Chapter 6: Discussion	KN	All
Chapter 7: Final Design and Verification	KC	All
Chapter 8: Conclusion and Recommendations	VG	All

Acknowledgements

The group would like to thank Professor Glenn Gaudette for his help and guidance throughout the project. In addition, the group would like to thank Katrina Hansen for her guidance, time throughout the year, resources, and assistance in executing experiments within the laboratory. The team also thanks Lisa Wall for her assistance throughout the MQP process and Biosurfaces, Inc. for scaffold sample production.

Abstract

Atrioventricular (AV) nodal block contributes to cardiovascular disease causing over 2,150 deaths in the United States each day. Due to the limitations of current pacemaker technology, there is a growing need for the development of a stem cell-based AV node bypass device to allow for normal cardiac function. The device must deliver electrical current from the atrium to the ventricle with minimal current loss and cell migration along its length. As the initial stage of device development, a PU/PET electrospun scaffold was designed and analyzed through the completion of this project.

Chapter 1: Introduction

According to the American Heart Association, cardiovascular disease (CVD) was the cause of 31.9% of all deaths in the United States in 2010, with over 2,150 Americans dying from CVD each day [1]. There are many types of heart conditions that contribute to making cardiovascular disease the number one cause of death in the United States [2]. One such condition is known as atrioventricular (AV) nodal block. AV nodal block interferes with the electrical system of the heart, which when functioning properly, controls and maintains a regular heartbeat in order to pass blood through the chambers of the heart and throughout the rest of the body [3]. In AV nodal block, the sinoatrial (SA) node, located in the atrium, is fully functional. However, the electrical signal that is propagated from the SA node is disrupted and unable to pass to the ventricle via the AV node. AV nodal block significantly affects heart rate and is normally detected through electrocardiograms [3]. While some people are born with AV nodal block, others develop the condition throughout their lifetime due to heart damage caused by other diseases, surgical procedures, or medications [3]. AV nodal block may cause fatigue, dizziness, fainting and can be fatal [3]. Thus, AV nodal block requires immediate treatment [3].

The current standard for treating AV nodal block is the implantation of an electrical cardiac pacemaker. An electrical cardiac pacemaker is an impulse generator that is implanted into the patient's chest. Electrodes, connected to two leads originating from the generator, are inserted intravenously into the heart to regulate abnormal heart rate [4]. The current cost for this device ranges from \$35,000 to about \$45,000 [5]. Despite the high cost of the device, there are about 300,000 pacemakers implanted each year in the United States as a means to treat abnormal node functions, such as AV nodal block [6].

There are various disadvantages associated with the use of an electrical cardiac pacemaker. One limitation of this device is its inability to exhibit an autonomic response when exposed to physiological stimuli, such as stress or exercise [7]. Electrical cardiac pacemakers also require regular device testing and replacement for preventative maintenance. In addition, complications with implantation, including infections and lead displacement, can occur [7]. Electromagnetic interferences from the external environment or from other devices implanted in the body can interfere with pacemaker functionality. Finally, electrical cardiac pacemakers come in one size and are not adjustable for implantation in patients of various heart sizes and age groups [7].

The goal of this project was to design a self-sustaining, biocompatible AV node bypass mechanism that passes electrical current from the atrium to the ventricle to treat AV nodal block while overcoming the limitations of the current treatment method. The bypass mechanism, or “AV bridge,” utilizes fibrin microthread sutures seeded with human mesenchymal stem cells (hMSCs) to transfer the electrical current from the atrium to the ventricle. The seeded threads are encapsulated by a scaffold in order to insulate the current. The cellular-based AV bridge overcomes the limitations associated with electrical cardiac pacemakers through its physiological responsiveness to stimuli such as exercise or emotional stress by utilizing the signal naturally generated by the SA node. The fully developed bypass mechanism should be self-sustaining, requiring no external power source and eliminating the need for routine testing and replacement.

Chapter 2: Literature Review

2.1 Structure and Mechanical System of the Heart

The human heart is a hollow structure that is located posterior to the sternum and ribs, and anterior to the vertebral columns as shown in Figure 1 [8]. A healthy heart is about the size of a clenched fist, weighing about 250-350 grams [8]. The heart wall consists of three layers: the pericardium, myocardium and endocardium. The pericardium is the outermost portion of the heart that protects the vital organ. Directly inside the pericardium layer is the myocardium, which makes up the majority of the heart. On a cellular level, the myocardium primarily consists of striated cardiac muscle composed of cardiomyocyte cells that are responsible for the contractile function of the heart. The innermost layer of the heart wall, the endocardium, is a sheet of endothelial cells that allows for smooth blood flow throughout the heart [8].

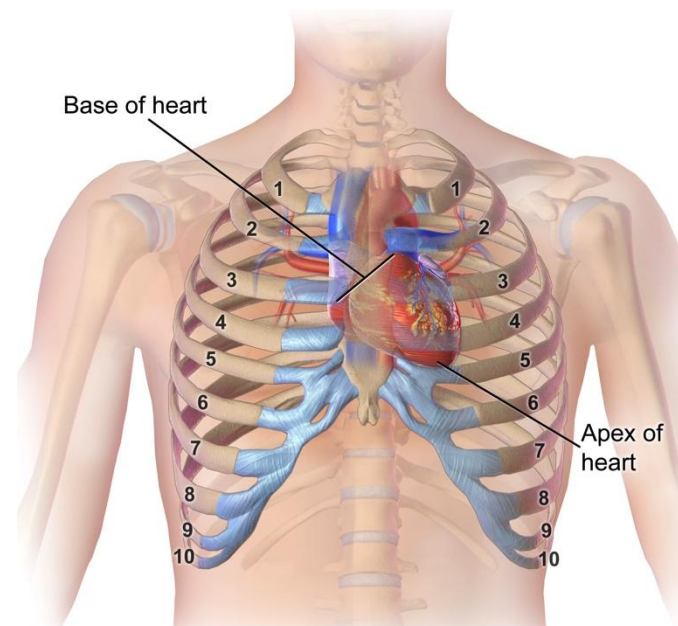


Figure 1: Heart location in relation to the rib cage and spinal column (Source: http://commons.wikimedia.org/wiki/File:Blausen_0467_HeartLocation.png)

There are four separate chambers in the heart: the right atrium, the right ventricle, the left atrium and the left ventricle as shown in Figure 2. The right and left chambers are separated by a muscular wall referred to as the septum [9]. The septum prevents the oxygenated blood within the left side of the heart from mixing with the deoxygenated blood within the right chambers. Specifically, the two atriums are separated by the interatrial septum, while the two ventricles are separated by the interventricular septum [8]. The atria and ventricles are separated by connective tissue, often referred to as the central fibrous body (CFB) or the fibrous skeleton of the heart [9]. This CFB functions as the insulator of electrical current and action potentials between the atriums and ventricles, which will be discussed in the following section.

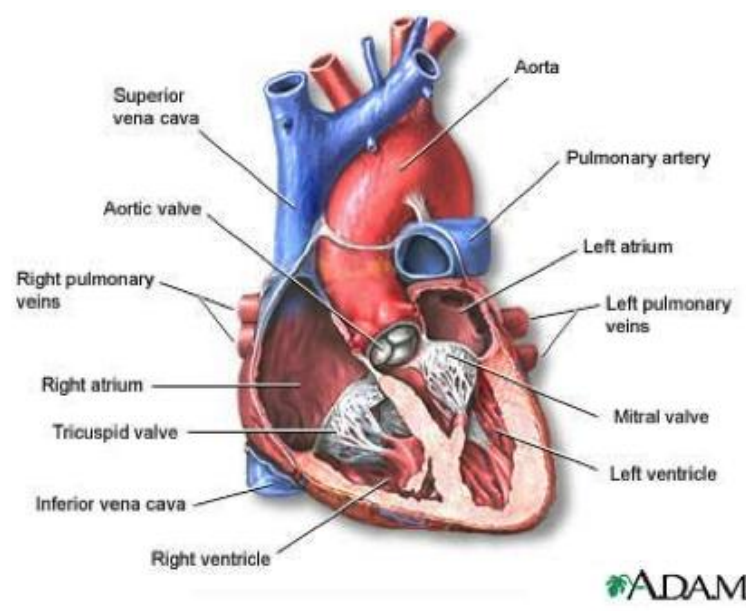


Figure 2: Diagram of the four chambers and valves of the heart (Source: <http://www.ohsu.edu/blogs/doernbecher/files/2012/08/heart-valves>)

The system of blood flow throughout the body is managed by the cardiac cycle of the heart. The two atria simultaneously fill and contract, sending the blood to the ventricles. Then, the two ventricles simultaneously fill and contract about 0.2 seconds later, sending the blood through the circulation systems of the heart, which will be described below [9]. Following the

contraction period, often referred to as systole, the atria and ventricles experience a relaxation period called diastole. The cardiac cycle is controlled primarily by pressure gradients present in the heart that cause the heart valves to open and close, managing the flow of the blood throughout the heart and body [8].

Blood flow throughout the body is controlled by two circulation systems of the heart, the pulmonary and systemic circulation systems. In the pulmonary circulation system, the deoxygenated blood enters the right atrium through the superior and inferior vena cava and is sent to the right ventricle through the tricuspid valve [9]. From the right ventricle, the blood is then sent through the pulmonary semilunar valve into the pulmonary artery, through which the blood is pumped to the lungs. While in the lungs, gas exchange between the blood within the lung capillaries and the alveoli occur, providing the blood with oxygen and transferring the carbon dioxide from the blood into the alveoli. The oxygenated blood then travels through the pulmonary veins and into the left atrium, where the systemic circulation system begins [9]. The oxygenated blood travels to the left ventricle through the mitral valve, where it is then pumped through the aortic semilunar valve and into the aorta. The aorta splits into branches and supplies oxygenated blood to all organs within the body. The organs retrieve the nutrients, including oxygen, from the blood, thereby deoxygenating the blood. This deoxygenated blood then returns to the right atrium and the pulmonary circulation system begins again [9].

2.2 Electrical System of the Heart

The electrical system of the heart exhibits ultimate control over the mechanical function of the heart. The electrical system of the heart relies greatly on pacemaker cells. Pacemaker cells are specialized cardiomyocytes that serve as the electrical impulse generating and conducting cells of the heart [10]. The contractile function of the heart is moderated by the electrical activity that is generated from the pacemaker cells within the SA node. The SA node, located in the

upper anterior of the right atrium, consists of the conducting pacemaker cells that generate the electrical impulse that is subsequently passed throughout the heart [11]. The electrical signal originates from the SA node, passes through the atrium walls, and is delivered to the AV node.

The AV node is a “compact spindle-shaped network of cells” [12] located in the right atrium below and posterior to the SA node [11]. The main cells that constitute the AV node are pacemaker cells and transitional cells [13], [11]. Transitional cells connect the specialized pacemaker conducting cells of the node with the cardiomyocytes in the atrium. With smaller and fewer gap junctions among the transitional cells of the AV node, the electrical signal is delayed by the node to allow for the complete emptying and closing of the atrium and the complete filling of the ventricles prior to ventricular contraction [13]. This delay is typically between 100-300 milliseconds [14], [15]. Aside from delaying electrical signal, the AV node has the ability to act as a backup pacemaker in the case of SA node malfunction [13]. Finally, the AV node is also responsible for transferring the current from the right atrium to the ventricles. The AV node is the only pathway for current transfer between the chambers, bypassing the insulating CFB [11]. In the case of AV node malfunction, electrical current is unable to propagate from the atrium to the ventricles via an alternative route.

The AV node collects the electrical signal generated from the SA node via the inferior nodal extension, which connects the node with the right atrium walls [11]. The signal passes through the AV node with slight delay and enters the Bundle of His. The Bundle of His is a collection of heart cells that collect the current from the AV node and ultimately pass the current to the ventricles. The Bundle of His splits into left and right bundle branches that are covered by a fibrous lamina that insulates the electrical current and prevents it from exiting the branches as it is propagated [11]. At the end of the fibrous covering of the bundle, the left and right branches

are referred to as the Purkinje fibers. The Purkinje fibers stimulate the cardiomyocytes of the ventricles, causing them to contract and pump blood throughout the body [11].

In summary, the electrical impulse that controls the heart beat is generated by the SA node, passed through the atrium walls to the AV node, through the Bundle of His and, finally to the Purkinje fibers that stimulate the cardiomyocytes of the ventricles to contract. Figure 3 below visually depicts this process.

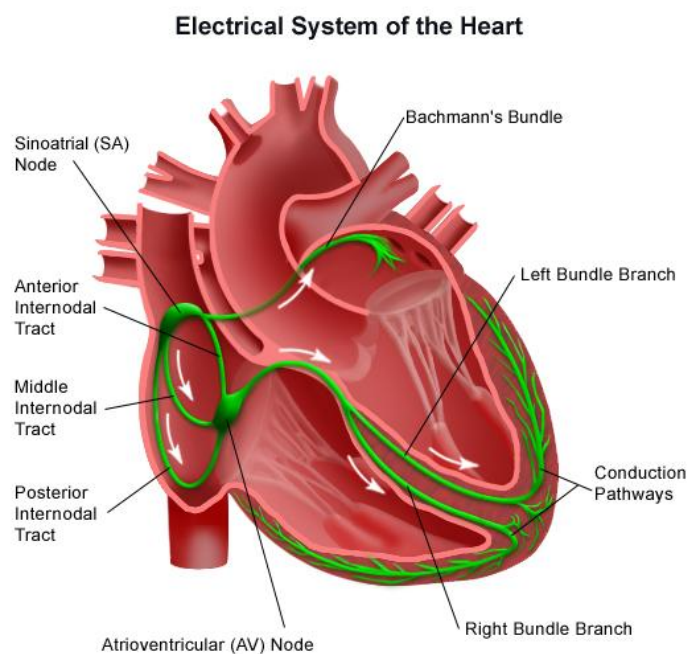


Figure 3: Electrical conduction pathway of the heart
(Source: http://weill.cornell.edu/cms/health_library/images/ei_0018.jpg)

2.3 Electrical Propagation through the Heart

As previously described, the contractions of the heart are stimulated and caused by the electrical current delivered to cardiomyocytes throughout the heart. On a cellular level, the cells able to pass the pacemaker current, also known as funny current (I_f), from cell to cell are what stimulate the heart's contractile function [16]. The cells are also able to pass ionic currents such as the calcium and sodium currents. An important aspect of the propagation of electrical current

throughout the heart is the cells' ability to communicate with one another. Communication between cells occurs through cellular connections called gap junctions. Gap junctions facilitate the exchange of ions between cells that allows for electrical and biochemical coupling. Gap junctions are formed between cells that contain the same connexin intermembrane proteins and are in close proximity to one another. These connexins are grouped together to form hemichannels that have the ability to link with other channels located on nearby cells [17]. Specifically, in human heart tissue, there are three types of connexin proteins, Connexin 43 (Cx43), Connexin 40 (Cx40), and Connexin 45 (Cx45). Cx43 is located in the ventricles, atria, and purkinje fibers. Cx40 is found in the SA node, atria, bundle branches, and the purkinje fibers. Finally, Cx45 is found in the SA and AV node, as well as the purkinje fibers [14]. The gap junctions formed by these connexins are able to efficiently pass the I_f and other ionic currents from one cell to another, allowing for the propagation of an action potential throughout the heart.

As stated above, electrical impulses are generated in the SA node, passed through the atrial wall to the AV node, and transferred into the ventricles. As the electrical impulse is propagated throughout the heart, the electrical potential of the cells is adjusted. The natural resting potential of a cell is approximately -90 mV [18]. When the surrounding potential reaches -70 mV, the cell is depolarized and the current is propagated from one cell to another. The change in the membrane potential is known as action potential [18]. The action potential is generated by the exchange of K^+ , Ca^{2+} , and Na^+ ions through selectively permeable ion channels and promotes cardiac muscle cells to contract and pump throughout the body [18].

The action potential consists of five phases as depicted in Figure 4 below. At -70mV, Phase 0 of action potential occurs. During this phase, the Na^+ channels initially open and the

positive sodium ions rush into the cell [18]. As a result, the inside of the cell becomes highly positive in comparison to its exterior environment. When the maximum positive voltage within the cell is reached, the Na^+ channels close and the fast K^+ channels will open in Phase 1 of action potential. Thus, K^+ ions exit the cell, causing a decrease in the voltage within the cell. During Phase 2 of action potential, Ca^{2+} channels open and the fast K^+ channels close. This creates a plateau in which the membrane potential does not change [18]. The steady potential prolongs the action potential in order to collect efficient signal needed to travel throughout the conduction pathway of the heart. In Phase 3, the slow K^+ channels open and the Ca^{2+} channels close [18]. This phase occurs in order to decrease membrane potential until the resting potential of -90 mV is reached. Finally, at Phase 4, the action potential is complete and the resting potential is maintained [18]. Each phase of action potential contributes to the passing of the I_f current, allowing for the cardiomyocytes of the heart to contract.

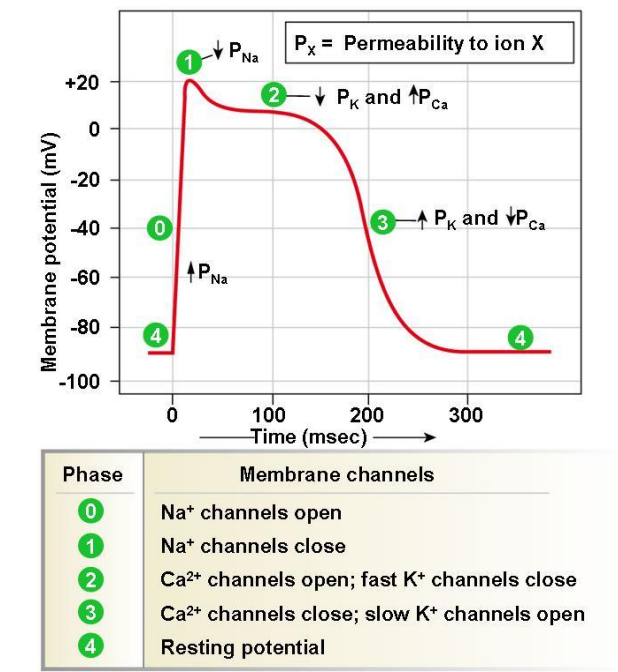


Figure 4: Phases of action potential generation displayed in a membrane potential versus time graph (Source: <http://www.austinctc.edu/apreview/PhysText/Cardiac.html>)

As mentioned previously, the funny current, I_f , is the current that paces the heart. This current is voltage dependent, allows for diastolic depolarization, and controls the overall excitability of the heart. The I_f requires a potential between -40 mV and -50 mV for its activation [16]. After an action potential occurs, the funny current is activated, slowly increasing the membrane voltage towards the threshold value at which another action potential can occur [16].

Hyperpolarization-activated cyclic nucleotide-gated (HCN) channels are intermembrane proteins that naturally occur in heart cells that assist in the generation of an action potential and the funny current. The HCN channels open when hyperpolarization is needed, but close during depolarization [6]. This ensures that the generation of current only occurs during Phase 4 of action potential and not during repolarization. Any type of current, including the ionic current or funny current, can pass through gap junctions between cells. However, cells without HCN channels or the equivalent cannot generate the action potential or funny current [19].

2.4 Heart Malfunctions: Arrhythmias and AV Nodal Block

There are various types of heart conditions that make cardiovascular disease a common cause of death each year. According to the 2014 *Heart Disease and Stroke Statistics* update produced by the American Heart Association, cardiovascular disease was the cause of 31.9% of all deaths in the United States in the year 2010, with over 2,150 Americans dying from CVD each day [1]. About 34% of these deaths occurred in patients below the current average life expectancy of 78.7 years old [1]. Various heart diseases contribute to these most recent statistics, including heart arrhythmias and heart blockages. These conditions interfere with the conduction system of the heart and frequently lead to irregular heartbeats [20].

The presence of arrhythmias in the heart interferes with the regularity of heartbeat pacing [20]. Generally, a heart affected with an arrhythmia is unable to pump adequate blood throughout the body. Symptoms associated with such heart conditions are fatigue, shortness of breath,

dizziness, and lightheadedness. These complications can ultimately result in damage to other vital organs, loss of consciousness, or even death [20]. Arrhythmias may interfere with atrial or ventricular pacing [20]. There are several types of arrhythmias that a patient may experience, including tachycardia and bradycardia. Tachycardia is an increased heart rate that often results from myocardial infarction. Bradycardia, or slow heart rate, may also be induced post myocardial infarction [20]. Bradycardia produces a slow, less frequent heart rate compared to a normal heartbeat [22]. Electrocardiographs (ECGs) are often used as a method of diagnosis for patients who experience tachycardia or bradycardia. ECGs record the electrical signal of the heart through electrodes on the thorax of the patient. Electrocardiographic signals of patients who experience ventricular tachycardias are small, with higher frequency compared to signals produced by hearts of normal pacing [21]. Both of these arrhythmias interfere with the regular pacing system of the heart and may require treatment with an electric cardiac pacemaker system depending on their severity [20]. ECG signals of these arrhythmias are shown below in Figure 5.

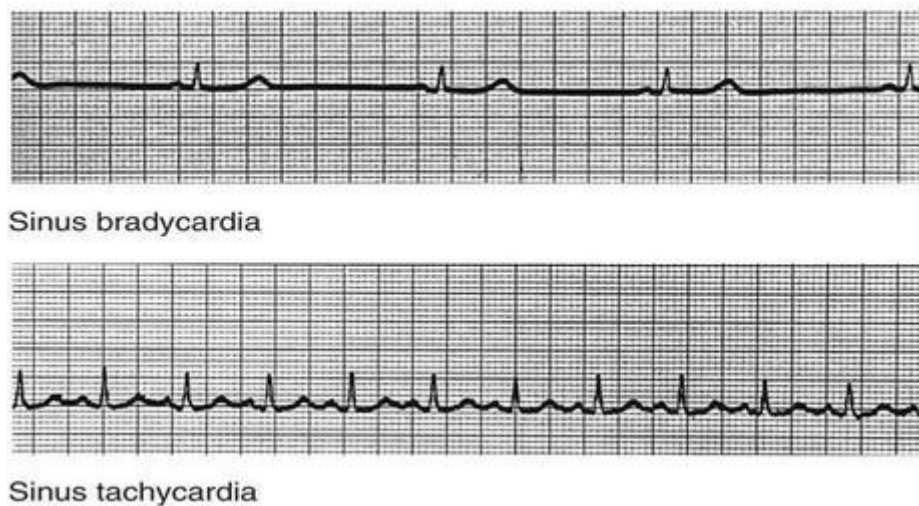


Figure 5: Bradycardia and tachycardia displayed via an ECG (Source: <https://humanphysiology2011.wikispaces.com/06.+Cardiology>)

Heart block is another condition that affects the electrical signaling of the heart, and therefore may be classified as an arrhythmia. Heart block can cause permanent or temporary conduction disturbance and can occur in various locations throughout the heart. The blockage of electrical impulse may occur within the atria during intra-atrial block, within the ventricles during intra-ventricular block, between the SA node and the atrium during SA nodal block, or between the atria and the ventricle during AV nodal block [23]. AV Nodal block, which is the abnormal conduction through the atrioventricular node, often induces ventricular bradycardia, or slow heart rate as previously described [20]. In AV nodal block, the sinoatrial node is fully functional. However, the impulse generated by the SA node is either unable to be passed to the ventricles or is conducted to the ventricle with immense delay. AV nodal block can occur in various locations throughout the conduction system of the heart, including the AV node itself, the Bundle of His, or the bundle branches [23].

Atrioventricular nodal blocks are classified by their degree of severity. In first degree AV nodal block, each atrial impulse is conducted to the ventricles and the ventricles are able to contract at a regular rate. However, the PR interval, or conduction time through the AV node, is elongated [23]. In second degree AV nodal block, atrial contraction, and therefore impulse conduction, is disrupted, intermittently or more frequently and at regular or irregular intervals [23]. The PR intervals associated with second-degree blocks may be fixed or elongated, causing intermittent or repetitive depolarization and contraction of the atria [23]. Third-degree nodal block is also referred to as complete nodal block and is the most severe. There is no atrial impulse conducted to the ventricles. Therefore, the atria and ventricles act independently at different rates, typically with ventricular rate less than 40 bpm [23]. Complete nodal block may be caused by congenital heart defects from birth that cause malfunctions [20]. A patient suffering

from AV nodal block may experience fatigue, dizziness, fainting, and even death if left untreated [3].

2.5 Electronic Cardiac Pacemakers

Currently, the only treatment of AV nodal block is the insertion of a cardiovascular implantable electronic device (CIED). The use of pacemakers as treatment for cardiac dysfunctions, including AV nodal block, is increasing worldwide, with a 55.6% increase in pacemaker implantation the United States from 1993-2009 [24]. The electronic pacemaker is commonly utilized to treat arrhythmias, conduction abnormalities, and heart failure. An electronic pacemaker is commonly implanted into the patient's chest through a minimally invasive procedure [7]. The placement of the overall device can be seen in Figure 6 below. A catheter is used to pass two leads, originating from the impulse generator, through the veins and into the atria surrounding the sinus atrial node [7]. This method of implantation eliminates the need for cracking open the sternum to perform open-heart surgery. On the end of each lead is an electrode, which delivers an electrical impulse to the heart, thus initiating and maintaining a regular heart beat [7].

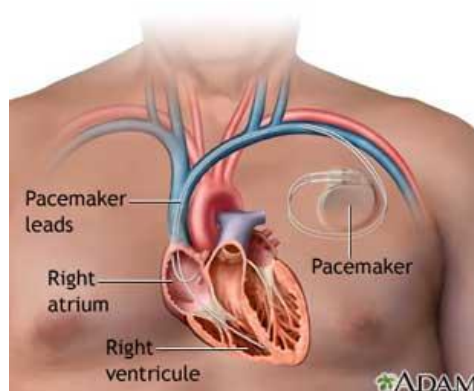


Figure 6: Image of the location of the electronic cardiac pacemaker

(Source:

http://www.uihealthcare.org/uploadedImages/UIHealthcare/Content/Health_Library/UI_Content/Heart_and_Vascular_Care/pacemaker.jpg)

Statistics show that there is a 5.6% annual average malfunction rate of pacemakers, illustrating one of the number of problems associated with the use of these devices [25]. Another limitation of cardiac electrical pacemakers is lack of physiological autonomic responsiveness, making the device unable to alter heart pacing in response to stimuli such as exercise or stress. While specialized rate-adaptive pacemakers have attempted to overcome this shortcoming, complications still arise [7]. For example, electrical pace-making units require consistent testing for functionality and replacement for reasons such as battery substitution [7]. Artificial pacemakers may also experience electromagnetic interference from the external environment [7]. Since these devices are not patient specific, both children and adults receive the same size pacemaker, which may cause complications during implantation and performance [7].

2.6 Autonomic Response

As stated above, one disadvantage of the electrical cardiac pacemaker is its inability to respond to the intrinsic control of the autonomic nervous system (ANS). In a fully functional heart, the ANS exhibits a strong influence on heart rate. Emotional and physical stimuli including fright, anxiety, and exercise activates the sympathetic system (SN) and induces an increase in heart rate [26]. In response to these stimuli, sympathetic nerve fibers release norepinephrine at the cardiac synapse, the location where electrical signal is transferred from the neuron to the cardiomyocytes [26]. Norepinephrine is a biogenic amine neurotransmitter and catecholamine hormone that is released and exhibits control over heart rate in response to emotional behavior [27]. The norepinephrine released by the nerve fibers binds to β_1 -adrenergic receptors located in the SA node. Thus, the threshold for an AP to occur is quickly reached, the SA node fires more rapidly, and heart rate is increased. Increased heart rate enhances contractile function of the heart and shortens the length of relaxation, as Ca^{2+} can be more readily available

to the contractile cells of the heart. As a result, end systolic volume decreases as heart rate increases [26].

Additional factors including age, gender, exercise, and body temperature also cause a response in heart rate. For example, resting heart rate decreases with age. The resting heart rate of a fetus (140-160 bpm) declines throughout ones lifespan. Additionally, the average heart rate in adult females (72-80 bpm) is generally higher than that of males (64-72 bpm) [26]. Exercise also has a large influence over heart rate. Throughout exercise, heart rate increases through the sympathetic nervous system as previously described. Systemic blood pressure increases during exercise while blood flow is directed to the active muscles of the body. The resting heart rate of one who is physically fit is generally lower than that of those who do not regularly perform physical activity [26]. Lastly, body temperature may also have an effect on heart rate. An increase in body temperature is accompanied by an increase in heart rate, as the metabolic rate of cardiac cells is enhanced. In contrast, a low body temperature decreases heart rate and metabolic activity of cardiac cells [26]. Electrical cardiac pacemakers are unable to respond to these stimuli. A cellular-based therapy in treatment of AV nodal block has the potential to act as an alternative treatment with autonomic response to various stimuli.

2.7 Potential Cell Types

There are many different cell types that could be considered for use in an AV node bypass mechanism. For example, the use of skeletal myoblasts has been investigated. Some advantages of this cell type include their high proliferation rate *in vitro*, their ability to remain in an undifferentiated state, and their ability to resist ischemic stress. Skeletal myoblasts also have a low risk of tumor formation and do not require treatment using immunosuppressants after injection into the human body [28]. However, despite all of these advantages, the major disadvantage of skeletal myoblasts is that they are unable to electrically couple with

cardiomyocytes [17]. It is vital that the cells of the AV bridge communicate with cardiomyocytes in order for the current to be passed from the atrium to the ventricles.

Two other options for use in an AV bridge are embryonic stem cells (ESCs) and induced pluripotent stem cells (iPSCs). ESCs and iPSCs are both capable of differentiating into pacemaker cells. Therefore, there is no need for the transfection of pacemaker genes, such as HCN gene channels, to generate current and prevent current loss along the length of the bridge. Additionally, ESCs have been shown to function properly when injected into porcine hearts [29]. iPSCs have been shown to be autonomically responsive *in vitro* [30]. In addition, iPSCs do not migrate, staying localized after delivery into the heart, which is beneficial in an AV bridge application [6]. However, there are limitations associated with the use of ESCs and iPSCs. For example, ESCs and iPSCs require the use of immunosuppressants post implantation or injection to prevent rejection [29], [30]. Specifically in iPSCs, gene memory could result in the inability of the cell to express the genes of interest [6]. Also, iPSC do not contain the necessary connexins to allow for coupling with cardiomyocytes [31]. Specifically with ESCs, there are many ethical controversies surrounding the use of embryonic stem cells.

A final cell option for this application is human mesenchymal stem cells (hMSCs). These cells are typically found in bone marrow and have the ability to differentiate into multiple cell types [32]. These cells have been shown to be safe to use and to contain the necessary connexins to form gap junctions with native cardiomyocytes [35]. Gap junctions are vital for cell-to-cell communication, allowing for the current to be successfully passed. hMSCs are also biocompatible, genetically stable, and have the ability to release growth factors to promote healing within the heart [35]. Research has shown that hMSCs have a high proliferation rate *in vitro*, making it plausible to generate the amount of cells needed to deliver a therapeutic dose

[36]. However, hMSCs have a tendency to migrate from the point of insertion, causing a potential problem in their use for an AV node bypass mechanism [37].

In order to generate current and prevent current loss along the length of the bridge, skeletal myoblasts and hMSCs require the addition of HCN gene channels through gene therapy. Past research has shown that HCN channels can be successfully added to hMSCs. The genetically altered hMSCs were then successfully shown to propagate an action potential that produced a heartbeat when coupled with cardiomyocytes [38], [35]. However, HCN channels are not required for hMSCs to form gap junctions with one another and pass electrical current from cell to cell. The main advantage of using HCN transfected cells within the stem-cell based bridge would be to generate current to accommodate for current loss as it is passed along the length of the device.

There is limited prior research indicating how the addition of the HCN channels will affect the proliferation of hMSCs. In one study, it was shown that *in vitro*, the proliferation rate was slow and the hMSCs only divided five times over 44 days [40]. This could be a disadvantage with the use of hMSCs and would require careful consideration and testing when determining the amount of cells needed for an AV node bypass mechanism [40].

2.8 Fibrin Microthreads

Fibrin microthread scaffolds are advantageous for various therapeutic applications, and can be considered for use in the AV bridge. Fibrin microthread scaffolds are utilized for their biocompatibility, and thus illicit minimal immune response when implanted into the body [41], [42]. Specifically, fibrin is a natural structural protein that is present in the early stages of wound healing [41], [42]. Throughout natural wound healing, fibrin promotes cell migration, attachment, and proliferation through cell-signaling properties that attract cytokines and growth factors to the site of injury [41], [42]. The presence of these cytokines and growth factors then

enhance cellular repopulation and tissue regeneration [42]. Additionally, fibrin contains RGD binding sites required for cell adhesion throughout tissue regeneration [41], [43]. Single fibrin microthreads have limited mechanical strength, which can be increased when braided or woven together to form bundled microthread sutures [42], [41].

The U.S. Food and Drug Administration has approved the use of fibrin scaffolds for medical applications, including surgical adhesives [43]. These scaffolds have been used to prevent blood loss and promote granulation tissue formation by guiding the migration and proliferation of fibroblasts [42]. Bundles of fibrin microthreads have also been utilized for their ability to form microenvironments that are similar to those present under physiological conditions [44].

The fibrin application that will be utilized to deliver hMSCs to the heart to treat AV nodal block are fibrin microthread sutures. Individual fibrin microthreads are self-assembled structures that are produced through a co-extrusion process from solutions of fibrinogen and thrombin [42]. The fibrinogen solution is commonly obtained from bovine plasma and dissolved in HEPES buffered saline [42]. The thrombin solution is also obtained from bovine plasma but diluted in calcium chloride solution [42]. The solutions are extruded through polyethylene tubing into a bath of HEPES solution [42]. During the co-extrusion process of the solutions through a blending applicator tip, thrombin cleaves a peptide on the fibrinogen molecule to induce fibrin polymerization and the assembly of microthreads [42]. The resulting threads of about 100 μm in cylindrical diameter remain in the HEPES bath for about 15 minutes before being air-dried under the tension of their own weight [45], [42].

After being dried, the threads can be bundled together into sutures for increased strength and seeded with hMSCs for delivery into the heart. Previous studies have produced fibrin

microthread sutures composed of 12 intertwined fibrin microthreads, resulting in about 8 cm long bundles [46]. These bundles were then cut into 4 cm lengths, threaded through a surgical suture needle and folded to produce a 2 cm long and 24 thread bundle suture [46]. Each suture contained about 5903 ± 1966 hMSCs/cm suture length after being seeded within a rotator [46]. Although the degradation rate of fibrin microthreads is relatively fast when exposed to physiological environments, it has the potential to be adjusted through UV or chemical crosslinking [47].

Through various cell-seeding techniques, such as static and dynamic cell seeding, hMSCs can be seeded onto fibrin microthread sutures [48]. It has been demonstrated that hMSCs maintain viability and their ability to proliferate when seeded on fibrin microthreads [43]. It has also been observed that cells seeded onto microthread bundles align along the longitudinal axis and within the grooves between individual threads [47]. Physical and chemical alterations of microthread bundles can increase the density of hMSCs seeded. For instance, microgrooves controlled by individual thread diameter within a bundle and patterned grooves stamped onto the threads can increase the surface area on which the cells can bind [41], [49]. Chemically, fibrin microthread sutures may be altered with additional cell adhesion molecules such as fibronectin and RGD peptides [42]. Due to their strong influence on cell adhesion, alignment, and orientation, fibrin microthreads have been used to aid in the delivery of stem cells [42]. In a previous study performed by Guyette, et. al., it was concluded that threads have a significantly higher delivery efficiency ($63.6 \pm 10.6\%$) into the left ventricular wall compared to intramyocardial injection ($11.8 \pm 6.2\%$; $p < 0.05$) [46].

2.9 Hollow Tubule Fibers

One developing technology that has the potential to be utilized in the AV node bypass mechanism is the hollow tubule fiber. The use of hollow fibers is being explored for tissue

engineering applications including regenerative medicine at institutes such as the University of Bath of the United Kingdom [50]. Hollow fiber tubules have proven to be successful, cell-scaffold constructs in regenerative applications including large bone defect augmentation and cell delivery to infarcted myocardial tissue [50]. In tissue engineering, there is a growing need for culturing cells within 3D, *in vivo*-like environments as opposed to flat, 2D standard tissue culture plates. Hollow tubules provide microenvironments for encapsulated cells that mimic *in vivo* conditions, functioning similarly to porous blood capillaries [50]. Another advantage of hollow tubules is the high surface area to volume ratio, increasing the amount of cells seeded and enhancing their ability to expand with little population variation [50]. In regenerative applications, different cell types may be cultured on the internal or external surface of the fiber [50].

The physical structure of hollow fiber tubules is dependent upon manufacturing properties that can be adjusted in relation to its intended use. For example, the permeability of the tubule can be altered to create a minimally resistant barrier between the cells seeded inside the scaffold and the external environment [50]. In addition, the structural, mechanical and topographical aspects are dependent upon manufacturing factors including, but not limited to, the polymer used to create the tubule [50]. These factors can be altered to enhance biocompatibility of the scaffold, cell number, and cell growth when implanted *in vivo* [50]. Tubules with different structural properties have been utilized to deliver drugs and growth factors for tissue regeneration [50].

Despite the advantages of hollow fiber tubules, there are also some associated limitations. For example, seeding cells within the tubule interferes with visual inspection of the cells inside [50]. The material composing the tubule may be unsuitable for initial cell attachment to the

scaffold, thus resulting in cell expansion [50]. Currently, there is no standard operating procedure to ensure desired success, as operation and function is heavily dependent on the cell type utilized and the final application of the tubule [50].

2.10 Electrospinning

Electrospinning of natural or synthetic polymer-based materials has been proven to be an effective and inexpensive method for scaffold production. This process can produce nanofibers of diameters as small as the nano-range, where other production methods are limited in this size range [51]. Typically, the fibers produced range from 5 to 500 nm in diameter [52]. Electrospun polymeric fibers have been characterized previously using scanning electron microscopy as shown in Figure 7, along with atomic force microscopy, X-ray diffraction and various other methods [53]. These nanofibers are then woven into a larger structure, such as a scaffold.

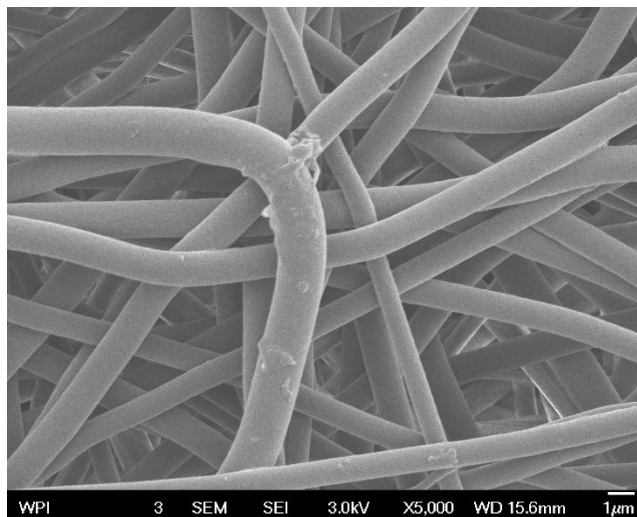


Figure 7: Scanning electron microscopy image of polymeric fibers produced via electrospinning

Electrospinning is based on the self-assembly of nanofibers due to electric charges and forces. The basic set-up of the electrospinning process can be seen in Figure 8 below. Briefly, a syringe filled with the polymeric solution contains a metal electrode that is connected to a power

supply capable of producing high voltages. In addition, there is a collecting metallic plate, whether cylindrical or flat, set a specified distance away from the syringe connected to the power supply. Once the voltage is applied, the syringe extrudes the solution, which then develops into fibers. These fibers are then collected on the plate to create the desired structure or scaffold.

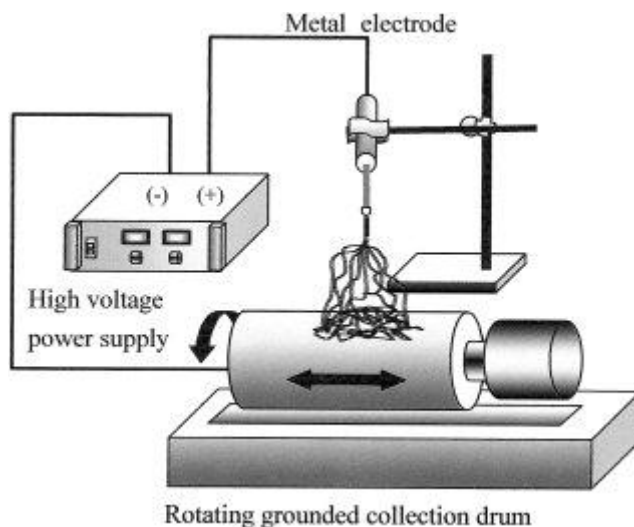


Figure 8: Diagram of the electrospinning process [52]

There are a number of advantages of the electrospinning process in scaffold development. First, this process is generally considered easy and simple to accomplish [52]. Secondly, scaffolds produced via electrospinning allow for a high surface area based on the porosity of the structure produced [52]. However, the control of the porosity of the scaffolds can be challenging, which is can be considered a drawback of this method. Third, electrospinning allows for the production of highly porous membranes, if desired, while also maintaining the structural integrity of the material [53]. Lastly, there are a number of parameters that can be controlled to alter the final product including spin time, voltage, solution concentration and distance between the syringe and collecting plate. These alterations can contribute to the control of the surface topography, fiber diameter and pore size [51].

2.11 BioGlue®

BioGlue® Surgical Adhesive, developed by CryoLife, is a medical adhesive solution that can be used to seal components of polymeric scaffold materials together. BioGlue® is composed of purified bovine serum albumin (BSA) and glutaraldehyde. The combination is non-toxic when applied within the body [54]. A bi-sectional syringe, seen in Figure 9, dispenses the two reagents and allows them to fully mix in the applicator tip. The controlled delivery system eliminates the need for manual mixing or solution preparation, as the syringe is self-contained, easy to use, and disposable. After extrusion, the solution polymerizes within twenty to thirty seconds and reaches maximum strength within two minutes [54]. BioGlue® degrades via proteolysis, and must be kept within a moist environment after application. This medical adhesive can be used as an effective method for surgical repair in place of sutures, staples or electrocautery. Some of the potential soft tissue applications of BioGlue® within the body include cardiac, vascular pulmonary, and genitourinary tissues [54].



Figure 9: Bioglue Surgical Adhesive, CryoLife. 2015. Web. 2 March 2015.
(Source: <http://www.cryolife.com/products/bioglue-surgical-adhesive>)

2.12 Heat Sealing

The application of heat is an alternative method for sealing one thermoplastic to another. Components of polymeric scaffolds can undergo heat sealing in order to shrink the material to seal a gap or create a closed bond. Heat sealing can be performed using a direct contact method or applying heat at a specific proximately to a localized area in order to weld the thermoplastics together. While there are various sealers available for a wide range of applications, there are two

main types of heat sealing. Impulse heat sealers apply a pulse of energy to an area of interest, immediately followed by the cooling process [55]. Impulse heat sealing is recommending for use of thermoplastic materials including polyethylene, polyurethane, polyvinylchloride, pilofilm, polyvinyl alcohol, saran, nylon, polyflex, mylar, tyvek, etc. [55]. In contrary, direct or constant heat sealing involves constant heat application directly at the sealing site, forming contact with the material. Direct heat-sealing offers consistent levels of heat with the ability to penetrate thicker materials [55]. Materials such as coated aluminum foil, poly cell films, gusset bags, coated Kraft papers, waxed paper, cellophane, etc. can be used with constant/direct heat sealing [55]. A soldering iron, shown in Figure 10, is one type of fine tip heat source that can be used to seal small, sensitive materials.



Figure 10: J&L 60 Watts Soldering Iron
(Source: <http://www.amazon.com/60-Watts-Soldering-Iron-listed/dp/B0006NGZK0>)

2.13 Cardiac Catheter

With advancements in medicine and technology, minimally invasive procedures are often preferred by both physicians and patients. For example, a minimally invasive method used for accessing the heart is cardiac catheterization. A catheter may be utilized in both diagnostic and therapeutic applications. Recent catheterization research has focused on the delivery of cells to the heart wall for tissue regeneration [56].

In 2011, a group of Worcester Polytechnic Institute students pursued catheter advancement by delivering stem-cell seeded fibrin microthreads to the left ventricular wall. To do so, the team developed a novel catheter system in accordance with standard catheterization procedures [57]. The catheter consists of a novel needle and core design contained within a sheath on the distal end of the catheter [57]. The sheath is detachable and can easily be replaced in order for physicians to load hMSCs-seeded microthreads onto the device [57]. The sheath creates a physiological environment for the cell-seeded fibrin microthreads, acts as a barrier between the cells and the exterior environment, and promotes cell viability while loaded in the catheter [57].

The delivery mechanism of the catheter is located inside of the sheath [57]. The delivery mechanism consists of the outer needle and the inner core, reducing the shear forces exerted on the cells while being inserted to the endocardium [57]. The inner core is contained within the outer needle as seen in Figure 11. Prior to delivery, the threads are draped over the inner core and are exposed as the inner core is pushed forward through the needle [57].

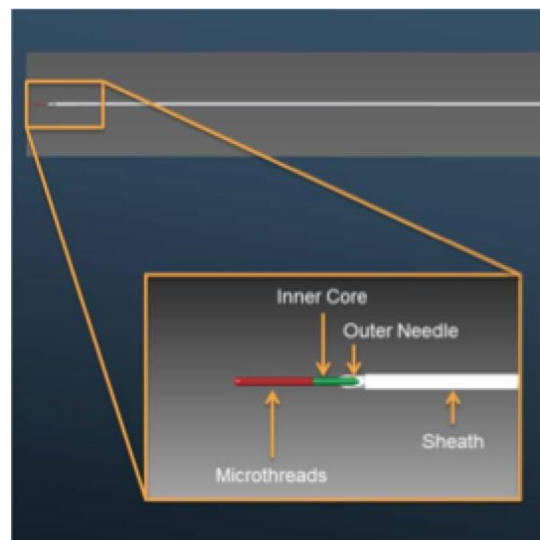


Figure 11: Delivery Mechanism of the Cardiac Catheter: Inner core and outer needle contained within the sheath [57]

While inserting the threads into the heart wall, the physician has control over the catheter on the proximal end [57]. The outer needle is exposed as the sheath is retracted upon entering the left ventricle through the femoral artery [57]. The outer needle and inner core are then plunged into the endocardial surface [57]. The inner core and threads are then pushed forward through the needle and are exposed within the heart tissue [57]. Once the inner core is deployed, the delivery mechanism is retracted from the infarcted tissue, leaving only the fibrin threads within the endocardium [57]. Finally, the needle is re-sheathed once the delivery mechanism has been removed from the ventricular wall [57]. Once the sheath is fully covering the outer needle, the catheter device is fully retracted from the body through the insertion pathway [57]. Insertion of fibrin microthreads into the heart wall is illustrated in Figure 12. Currently, there is ongoing development on the present catheter design. Ideally, the distal end of the catheter will be a detachable component in order to allow for pre-loading of the threads onto the inner core prior to the time of surgery.

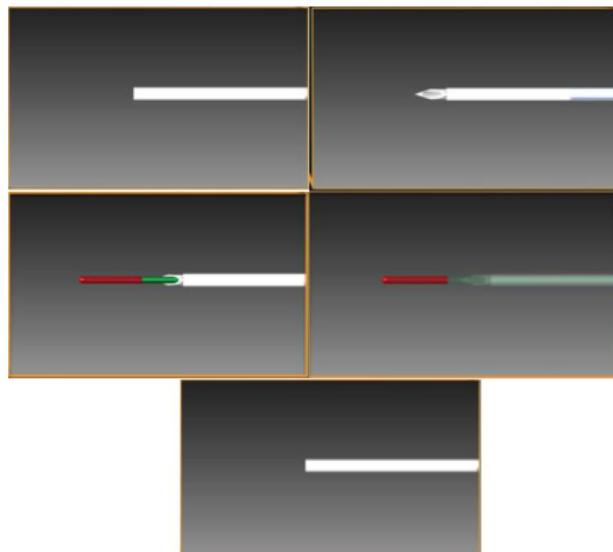


Figure 12: Insertion mechanism (read from left to right) [57]

Chapter 3: Project Strategy

3.1 Initial Client Statement

The original client statement provided to the team by Professor Gaudette is as follows:

Create a biological pacemaker for human use.

With current research being developed on a biological pacemaker, the team focused the project on an AV node bypass mechanism to electrically connect the atrium to the ventricle when the SA node is fully functional. Through thorough research, the team moved forward to develop objectives, constraints, functions, and specifications based on the use of fibrin microthreads seeded with hMSCs in order to develop an innovative bypass design. Through further discussion with the client and extensive background research, the team revised the initial client statement and began the design process of a fully developed AV nodal bypass device.

3.2 Objectives

Primary, secondary and tertiary objectives of the AV node bypass mechanism are depicted in an objectives tree located in Appendix I. Pairwise Comparison Charts (PCCs) were completed to rank the importance of each primary and secondary objective. The team members and the client individually completed the PCC to compare the primary and secondary objectives, found in Appendix II. Numerical results obtained by each team member were averaged and compared to the client's rankings to determine the final ranking of the importance of each objective. The results can be seen below in Tables 1 and 2:

Table 1: Results of PCCs comparing the team's average with Professor Gaudette's

Primary	Team Average	Client
Biocompatible	6	3
Physiologically Responsive	3.75	5
Self-Sustainable	3.875	5
Cost-Effective	0.375	0
Deliverable	3.375	3
Easy to Use	1.875	1
Reproducible	1.5	4

Table 2: Results of Secondary PCCs comparing the team's average with Professor Gaudette's

Secondary	Team Average	Client
Biocompatible		
<i>Immune Response</i>	2	2
<i>Disruption to Heart</i>	0.875	1
<i>Scar Formation</i>	0.125	0
Self-Sustainable		
<i>Passage of Nutrients</i>	1.75	2
<i>Outside Power Source</i>	1.5	2
<i>Withstand Cyclic Loading and Contractile Forces</i>	1.25	0
<i>Cell Balance</i>	1.5	3
Cost-Effective		
<i>Manufacturing Company</i>	0	1
<i>Insurance Company</i>	2	3
<i>Patient</i>	4	1
<i>Surgeon</i>	1	2
<i>Hospital</i>	2.5	3
Reproducible - Accuracy		
<i>Mechanically</i>	2	0
<i>Electrically</i>	1	2
<i>Biologically</i>	0	1

Through the completion of PCCs and discussion with the client, the primary objectives of the bypass mechanism are ranked in order of most to least importance: self-sustaining and physiologically responsive, biocompatible, reproducible, deliverable, easy to use, and cost-effective.

3.2.1 Self-Sustaining

Self-sustaining and physiologically responsive received the highest scores upon completion of the PCC, tying as the most significant primary objectives for the AV node bypass. Self-sustaining implies that the cellular device will be able to properly function when implanted inside the heart through optimal cell survival and sound structure without the need for an external power source. If the bypass mechanism is unable to maintain function once implanted into the heart, the electrical impulse will not be passed from the atrium to the ventricle and the device will fail.

In contrast to the electrical cardiac pacemaker, the bypass mechanism will not require an external power source. Therefore, routine device testing and battery replacement will not be necessary to maintain the function of the bypass throughout its lifespan. Due to the absence of an external power source, optimal cell balance within the bridge is crucial. The net proliferation and cell death rates must be balanced to provide optimal current propagation. This will ensure that the number of cells required to pass the signal from the atrium to the ventricle at a specified speed is continuously present and able to improve and maintain heart function. Furthermore, the device should allow for the passage of nutrients to the cells to promote cell survival. If the nutrients cannot reach the cells, the cells will not remain viable, the current will not be propagated through the heart, and the device will ultimately fail. Finally, the bypass mechanism should be able to withstand the natural cyclic contractile stress that the heart will exert on the bridge. Thus, the bridge must remain structurally sound after its implantation into the heart.

The most important secondary objective within self-sustaining is the passing of nutrients to the cells. This objective is followed by cell proliferation balance and functionality without an outside power source, both of equal importance. The least important objective is the ability to withstand the cyclic loading and forces naturally produced by the heart. The ranking of secondary objectives supports the importance of cell survival required for device functionality. To promote cell viability and survival, nutrients must be passed to the cells and waste must be removed from the cells within the bridge. An appropriate cell balance is necessary to ensure that an optimal amount of current is passed through the bridge. The absence of an external power source is of equal importance, making the bypass mechanism an improved treatment method for AV nodal block compared to the electrical cardiac pacemaker. Finally, it is important that the device withstands the forces exerted by the heart. However, this secondary objective is of least importance compared with previously ranked objectives as structural stability does not promote current propagation if viable cells are not present within the bridge.

3.2.2 Physiologically Responsive

In contrast to the electrical cardiac pacemaker, the AV node bypass mechanism should be physiologically responsive. The device should be able to pass a range of currents at different speeds in relation to the generation of current by the SA node in response to physiological stimuli such as exercise and stress. As one of the main objectives of the AV node bypass mechanism, physiological responsiveness is comparably significant to self-sustaining. Meeting this objective will improve current treatment methods for AV nodal block, such as the electrical cardiac pacemaker, adjusting heart rate according to physical and emotional stimuli.

3.2.3 Biocompatible

Biocompatibility involves the ability of the device to minimally interrupt natural heart function and ultimately avoid rejection when implanted into the body. Biocompatibility is the

third most important primary objective of the device and is a crucial component promoting optimal device function. However, there is a degree of incompatibility that will not interfere with device function. Therefore, minimal immune response, minimal disruption to the contractile system, and minimal scar formation may occur without affecting device function as long as the symptoms do not reach an incompatible threshold that causes the heart to fail.

When implanted into the body, the bypass mechanism should produce minimal immune response, with little inflammatory reaction and cytotoxicity. In the presence of significant immune response, the device would be rejected, leading to failure and presenting dangerous conditions to the patient. It is likely that a slight immune response may occur while implanting a foreign object into the heart. Due to the potential severity of harmful conditions that the patient could ultimately be exposed to, minimal immune response is the most important biocompatible objective the device meets.

Secondly, the device should minimize disruption to the natural contractile system of the heart. There can be a small degree of disruption to the contractile system; however, the heart should effectively pump blood throughout the body when the device is implanted. This is an important objective that allows the heart to perform normal contractile function with the implanted device present to assist in current propagation and regulating heartbeat.

Finally, the bypass mechanism should produce minimal scar tissue formation and overgrowth of collagen. Scar tissue and collagen overgrowth may interfere with the passage of current from the atrium to the ventricle through the bypass mechanism and lead to malfunction and device failure.

3.2.4 Reproducible

Another major objective that needs to be considered is the reproducibility of the device. It is important that the device produces uniform results and properties in terms of functionality and

manufacturability. Reproducibility encompasses the accuracy and precision of device functionality. It is ranked as the fourth most important objective because in order to prevent failure of the device, it is not necessarily important for the device to be easily reproduced. However, in order to function properly, it must produce accurate results in current propagation. Precise functionality and properties are important to consider if the device is to be mass-produced. It is concluded that the accuracy of the device is more important than its precision, as accurate properties directly relates to proper functionality in passing the current from the atrium to the ventricle.

First, the device must accurately pass the necessary amount of signal at an appropriate velocity with required delay to promote normal contractile function of the heart. This was considered to be the most important secondary objective based on the primary function to pass the current required to pace the heart. Secondly, the cellular-based device must consistently interact with the biological tissue surrounding the implantation site. Finally, it is least important that the bypass mechanism is produced to have accurate yield strength and fatigue failure based on intended design values to ensure that the device will not ultimately fail. This objective is least important because mechanical properties do not directly affect the ability of the device to pass electrical current. However, these properties must be accurately reproduced for every patient to ensure safety and proper function of the device.

As mentioned above, the precision of device reproducibility is important for mass marketing the device. If the device were to be mass-produced, the FDA and other regulatory agencies will require that the device have precise, standard manufacturing processes. However, this does not directly affect device functionality. In relation to mass-production, the manufacturing process of the device should utilize a consistent protocol in order to guarantee

that the same product is created each time. If various manufacturers cannot reproduce the protocol, a limited amount of effective bridges will be created and the device will therefore be utilized by a fewer amount of patients.

3.2.5 Deliverable

Another main objective that should be considered is the delivery of the device into the heart. Deliverable was considered to be less important than reproducible because it does not affect the way the device functions. The secondary objectives that relate to deliverable are minimally invasive, compatible with the current technology, and implantable. It is most important that the delivery method be minimally invasive to result in fewer potential complications, as well as a fast recovery time. This is most important because it directly affects the health of the patient. The second most important sub-objective is compatibility with current technology, referring to the fact that the device should use current methods and instruments developed for the delivery of devices to the heart. The use of current technology will eliminate the need to develop a new tool for delivery and would result in sooner marketing of the device.

3.2.6 Easy to Use

The next primary objective to consider is that the AV bridge should be easy to use. This objective is not of crucial importance because it does not directly affect the function of the device. Ease of use is less important than deliverability because the ease of use will not affect the health of the patient. There are two secondary objectives under ease of use: ease of implantation into the heart and the ease of assessing functionality of the device after implantation. Easy to use encompasses both the materials utilized and method of implantation. The materials that compose the device must be easy for a prep team and surgeon to handle and implant, ideally with minimally invasive techniques. Additionally, cardiologists must be able to easily assess the functionality of the device after implantation through a procedure that does not

require additional surgery. If the functionality of the device cannot be measured by a cardiologist years after implantation, then it will be difficult to ensure the health of the patient.

3.2.7 Cost-Effective

The final and least important primary objective for the AV node bypass mechanism is cost-effectiveness, which implies that the price of the bypass must be comparable to that of an electronic cardiac pacemaker currently on the market. The device needs to be reasonably priced to ensure it can be marketable. If there is a large increase in price compared to that of an electronic pacemaker, the value of the bypass should increase so that stakeholders are willing to pay more for the product. If the final product is too expensive and believed to not be worth its price, it will not be purchased. The ability to compare the price of the device to the price of the gold standard will vary depending on the targeted audience. Targeted audiences examining the cost of the device include the manufacturing company, insurance company, patient, surgeon and the hospital.

It was determined that the device should be most cost effective to the insurance company. The insurance company will be a primary stakeholder to the device because it will cover the cost of the bypass. If the insurance company does not believe the device is worth its' cost, they will not cover the expense for the patient. The hospital is the second most important audience in terms of cost-effectiveness of the device. If the hospital does not believe the device is cost effective, they will not carry the product and the bypass will not be an option of treatment for the patient. The manufacturing company is the third most important when considering cost-effectiveness. The main priority of the manufacturing company is to make a profit from the mass production of the device. If the device is too expensive, they will not make a profit and will not want to manufacture the AV node bypass mechanism. The patient was ranked of little importance in terms of the cost effectiveness of the device. While it is important for the patient to

believe the device is valuable, they will not be typically paying for the cost of the device themselves. Finally, the cost-effectiveness to the surgeon is least important because they do not have much concern over the cost of the device.

3.3 Functions and Specifications

In order to successfully meet the aforementioned objectives of the project, specific functions of the developed AV node bypass system are needed. Four overall functions of the system were developed:

- 1. Must receive, transmit and deliver current.*
- 2. Must minimize the loss of current transferred via the bypass system.*
- 3. Must minimize cell loss.*
- 4. Must not disrupt native heart function.*

3.3.1 Must receive, transmit and deliver current

With a malfunctioning AV node, the electrical conduction of the heart cannot be collected, transmitted or delivered to the ventricles. Therefore, the bypass system first needs to collect the electrical current from the SA node in the atrium in order to stimulate the bypass system and allow for continuation of action potentials throughout the length of the bridge. The bridge will contain an appropriate amount of human mesenchymal stem cells, which collect and pass the current through gap junctions between the seeded hMSCs and the native cardiomyocytes. By allowing for gap junction formation between the transfected hMSCs and native cardiomyocytes, the current will be able to be collected and passed throughout the bridge through the gap junctions between the cells [6]. The presence of the HCN channels in the hMSCs, which couple with the native cardiomyocytes, will allow for the generation of current along the bridge in the case of current loss which will be discussed further in a later section.

The end of the bypass bridge must be connected to the cardiomyocytes in the atrium to collect the current and stimulate the bypass system. The bridge must then be able to transmit the current from a point in the atrium to a point in the ventricle. As recommended by Professor Gaudette, the minimal bypass distance is 2 cm in order to bypass the central fibrous body. While the natural conduction velocity in the AV node is about 5 cm/s, the conduction velocity of the bypass system should be between 25-100 cm/s, per Professor Gaudette's request, in order to account for the longer distance travelled by the bridge in comparison to the natural length of the AV node [13]. The bypass mechanism should also account for the natural delay of a functioning AV node, which is approximately 100-300 ms [14], [15]. Finally, the bypass system must be able to successfully deliver the current to the ventricle via the gap junctions formed between the hMSCs and native cardiomyocytes in the right ventricle.

3.3.2 Must minimize the loss of current transferred via the bypass system

The electrical current propagated through the bypass device should pass primarily in the longitudinal direction and should be limited in loss of current in the radial direction. The loss of current in the radial direction would result in an inefficient conduction of the current to the ventricles. Therefore, the hMSCs must be encapsulated by an insulating scaffold that minimizes the loss of current.

The encapsulating scaffold ends should have a pore size of approximately 2.0-2.5 μm in order to allow for proper exchange of nutrients through the bridge to maintain cell viability, while also containing the current [58]. In addition, this pore size was calculated by a previous Worcester Polytechnic Institute Major Qualifying Project team to be small enough to prevent hMSCs from migrating through as these cells have a natural affinity to migrate [37], while still allowing the hMSCs to form gap junctions with the native cardiomyocytes. These gap junctions are vital in collecting the current from the atrium and delivering the current to the ventricle.

As mentioned above, the use of HCN channel transfected hMSCs should allow for the generation of current along the bridge if coupled with native cardiomyocytes. This should aid in the maintenance of the current along the bridge if any current is lost in the radial direction.

3.3.3 Must minimize cell loss

The bypass system must minimize cell loss throughout the manufacturing, implantation and lifetime of the bypass bridge. Throughout these processes, the bridge needs to maintain a certain number of viable cells in order to efficiently pass current from the atrium to the ventricle once it is in place in the heart. As agreed upon with Professor Gaudette, the order of importance of these three processes is transplantation, lifetime, and manufacturing. It is most important to minimize cell loss during the transplantation of the device into the heart because this is the stage in which there is the highest risk of losing cells while being unable to replace them thereafter. The method of delivery of the bypass system will be controlled, which ultimately controls the cell loss during this process. Secondly, the minimization of cell loss during the lifetime of the design is important because the loss of cells during this process calls for additional surgery to replace the cells or bypass system as a whole to maintain the functionality of the device. However, there is less control over this process in comparison to transplantation. Finally, the manufacturing of the complete bypass system must be controlled to minimize cell loss. This is least important due to the manufacturer's ability to replace lost cells at this point in time before implantation.

3.3.4 Must not disrupt native heart function

Finally, the AV node bypass system must cause minimal disruption to the functionality of the native heart. This system must not disrupt the contractile system of the heart, must not interrupt the mechanical function of the heart and must not produce an immune response by the heart.

3.4 Constraints

There are multiple identifiable constraints that were taken into account throughout the project design process: the overall safety of the device, the project budget, and the project time-span.

3.4.1 Safety

In terms of device design, safety acted as a key constraint. The AV node bypass must be safe, as it cannot illicit harmful, cytotoxic effects or be rejected when implanted into the human body. Factors, such as the amount of current conducted along the bypass mechanism, were carefully considered to ensure safety of the device and ultimately maintain the health of the patient. The material composition and subsequent degradation byproducts produced by the encapsulating scaffold also required consideration. The material and chemical byproducts could not cause harmful effects to the patient or compromise heart function.

3.4.2 Project Time-Span

Another constraint is the short time period during which this project must be completed. Specifically, the bypass mechanism was produced during the academic school year, extending from August 2014 to April 2015. All product development, design testing and data collection was completed by mid-April in order to report and compile final results by the project completion deadline in April 2015.

3.4.3 Project Budget

The limited budget of \$156 per team member, totaling \$624 in total for an MQP team of four members, was a constraint throughout the completion of this project. The cost of the Goddard Hall lab fee, prototype materials, including scaffold and testing materials, and final design materials had to be incorporated into the \$624 budget. All fees required for project design and testing aspects must be included within the \$624 total budget.

3.5 Revised Client Statement

In considering the developed objectives, constraints, functions and specifications, a revised client statement was developed to expand upon the original statement. This statement is as follows:

*Design and develop a **self-sustaining, biocompatible** AV node bypass mechanism that electrically connects the atrium to the ventricle. The bypass should be a minimum of 2 cm in length and have a conduction velocity between 25-100 cm/s. The bypass should make use of **fibrin microthreads** seeded with **hMSCs** to pass electrical current with an **encapsulating scaffold** around the threads to insulate the current. There should be a delay in conduction from the atrium to the ventricles similar to that of the AV node delay of approximately 100-300 ms. The bypass should be **physiologically responsive** to stimuli and have the **mechanical stability** to withstand cyclic loading of the contracting heart.*

3.6 Further Project Approach

Through further understanding and discussion of these developed objectives, constraints and functions, the team developed conceptual designs and preliminary designs through brainstorming activities and analysis, as will be discussed in *Chapter 4*. Each design was analyzed in order to determine parts of the device that needed to be tested in order to verify the functionality of the designs. These determined tests were run and allowed for the team to deem a final design of the AV bypass mechanism.

Chapter 4: Alternative Designs

Taking into consideration the aforementioned objectives, constraints, functions and specifications, the team developed a number of design concepts that would function as an AV nodal bypass mechanism. The team began this process with a brainstorming session in which each function was analyzed and conceptual methods of achieving them were determined. For example, the current could be collected from the SA node similar to how a plug collects electricity from a wall socket. Important ideas drawn from the brainstorming process are listed below in Table 3.

Table 3: Brainstorming activity results for the first three functions

	Idea 1	Idea 2	Idea 3	Idea 4
Receive, transmit and deliver current	Socket (Collect/Deliver)	Funnel (Collect/Deliver)	River (Collect/Transmit/Deliver)	Wire (Transmit/Deliver)
Minimize loss of current	Wire	Mesh	Myelin Sheath	
Minimize cell loss	Blood vessel diffusion	Skin		

4.1 Conceptual Designs

To begin the design process of developing the AV nodal bridge, conceptual designs were developed with the brainstorming ideas shown above in mind. The conceptual designs represent the beginning stage of determining the optimal final design. Each of the following conceptual designs includes a combination of fibrin microthreads, hMSCs and an encapsulating scaffold.

4.1.1 Primary Conceptual Designs

As shown in Figure 13, the primary conceptual designs consist of three versions of the bridge in which the fibrin microthreads seeded with hMSCs protrude out of the ends of the encapsulating scaffolds. The ‘funnel’ design consists of a number of threads protruding out of the scaffold in a funnel formation. This was seen as beneficial in terms of collecting current from a number of areas in the atrium and distributing the current in a similar fashion in the ventricles. The bridge would be able to collect the current due to the gap junctions formed at the ends of the scaffold between seeded hMSCs and native cardiomyocytes. The current would be passed along the bridge via gap junctions between the seeded hMSCs. This is displayed in Figure 13 and Figure 14 of conceptual designs.

Second, the ‘socket’ design in the center of Figure 13 imitates a plug and electrical socket, as the bridge similarly collects electrical current from two locations in the atrium and distributes to the ventricles in a similar fashion. However, there are fewer places from which the socket design can draw current from in comparison to the funnel.

Third, the bundle design on the right of Figure 13 is a simple bundle of microthreads seeded with the hMSCs within an encapsulating scaffold.

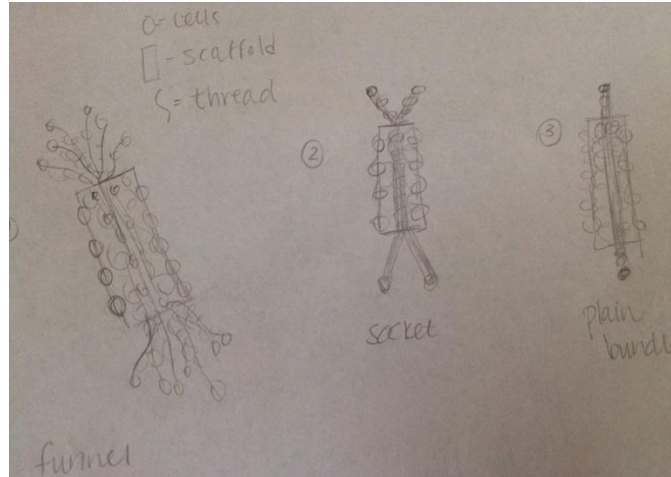


Figure 13: First conceptual designs - funnel (left), socket (center) and bundle (right).

Upon analyzing the primary conceptual designs, it was determined that the amount of fibrin microthreads and cells protruding from the scaffold would not meet the function of minimizing cell loss. With the purpose of the scaffold to encapsulate the cells and minimize migration of hMSCs, the team determined there must be minimum to no exposure of the cells to the surrounding environment.

4.1.2 Secondary Conceptual Designs

Taking the aforementioned minimal cell loss requirement into consideration, a secondary group of conceptual designs were developed as shown in Figure 14. The general ideas of the designs remain the same as the primary designs, with the exception of the scaffold extending further to allow for less cell exposure. This would allow for minimal cell loss and migration as there are fewer cells exposed in the atrium and the ventricle, therefore decreasing the amount of cells that may migrate away from the bridge. However, the threads and some cells still protruded from the scaffold, leaving room for improvement upon the designs.

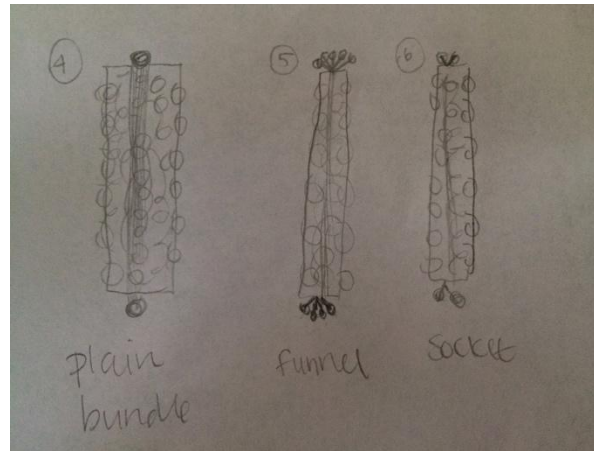


Figure 14: Second conceptual designs: bundle (left), funnel (center) and socket (right).

4.1.3 Final Conceptual Designs

The final conceptual design was developed in order to completely encapsulate the fibrin microthreads and hMSCs within the scaffold. The only exposure of the cells to the environment would be through the gap junctions between the hMSCs and native cardiomyocytes through the porous encapsulating scaffold in order to collect and deliver the current. The team believed this to be the ideal conceptual design with which to move forward in the development of preliminary designs of the AV nodal bridge. The design could be applied to the plain bundle, funnel and socket designs described above. Figure 15 below displays this design in the funnel styled option.



Figure 15: Final conceptual design in the form of the funnel scaffold.

4.2 Preliminary Designs

Following further discussion between the team and the client, preliminary designs were developed to account for cell loss accompanying the conceptual designs. The client brought to the team's attention the function of containing the current throughout the bridge. In the conceptual designs, this function was not properly considered. The preliminary designs reflect the consideration of this function, as the designs only allow for gap junction formation in the portions of the bridge that will be utilized collect and deliver current. The center portion of the bridge will inhibit gap junction formation in order contain the current and cells, while allowing for nutrients to diffuse into the bridge to maintain cell viability.

The preliminary designs show two sections of the bridge distinguished by different pore sizes and thicknesses within the scaffold. Larger pores were located on the ends of the scaffolds to allow for the gap junction formation between the seeded hMSCs and native cardiomyocytes. The remaining, center portion of the scaffold had smaller pore sizes to inhibit this gap junction formation. The developed preliminary designs are displayed and discussed below in reference to the key shown in Figure 16.

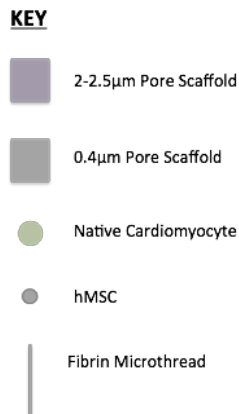


Figure 16: Key for the preliminary design images shown below.

An additional method of minimizing cell loss was considered in the preliminary designs. Each of the preliminary designs described have all ends of the scaffold sealed. It is believed that by sealing the ends of the scaffolds, the cells will have a decreased risk of migrating from the threads or scaffold. The method of sealing will be discussed further in a later section.

Overall, the two groups of preliminary designs described below present feasible design options for the development of a final design.

4.2.1 'Flattened Straw' Designs

After presenting the conceptual designs to the client and discussing more within the team, the possible concern of excess space within the scaffold was raised. Excess space may create microenvironments that can promote bacterial growth within the scaffold. This was undesirable for the AV nodal bridge, as bacteria may cause an unwanted immune response within the body. Therefore, two preliminary designs were developed to be flat, as shown in Figure 17 below.

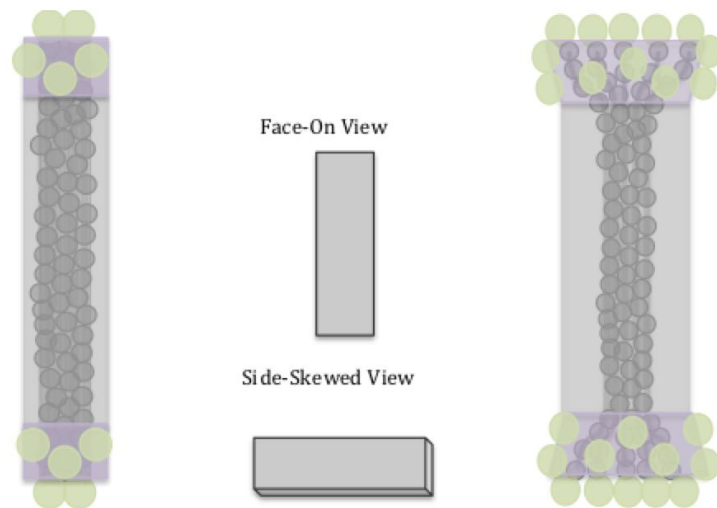


Figure 17: 'Flattened Straw' plain bundle (left) and 'Flattened Straw' funnel (right) preliminary designs.

The primary concern with this design was implantation within the heart. With the team focusing on a minimally invasive catheter delivery of the device, it was important to consider that these preliminary designs would be unable to be delivered via catheter, as they are not in cylindrical form.

The funneled ends of the preliminary design shown above also presented a constraint in catheter delivery, as the cylindrical catheter would be unable to account for a wider diameter of the funneled ends. If the design were to be altered to allow for the funneled ends to meet the maximum diameter the catheter can withhold, this would limit the amount of space for fibrin microthreads and cell seeding. Having the appropriate amount of hMSCs to allow for the propagation of current was a more important objective than the delivery of the bridge as seen in the Pairwise Comparison Chart. Therefore, the diameter alterations that accompany the funneled design would not be acceptable.

The method of fabrication of the funneled ends is also a major concern of the funneled end preliminary design shown in Figure 17. The methods of scaffold fabrication under consideration will be discussed in a later section. However, each method of fabrication will present a challenge in developing a funneled-like scaffold.

4.2.2 Cylindrical Designs

Considering catheter implantation of the final design, two preliminary designs were developed to be in cylindrical form as shown below in Figure 18. These two designs were similar to the aforementioned flattened straw designs, however they were in cylindrical form in order to account for the delivery mechanism.

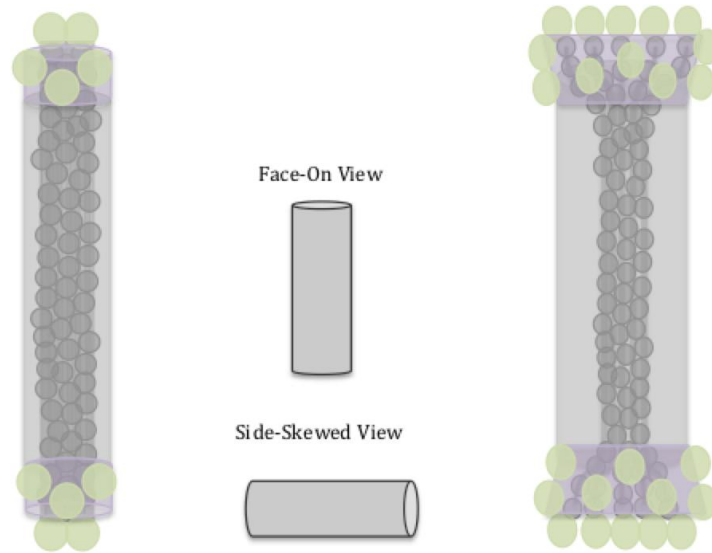


Figure 18: Cylinder plain bundle (left) and cylinder funnel preliminary designs.

After analyzing both groups of preliminary designs with the team and client, primary concerns of bacterial growth in microenvironments and the use of funneled ends were brought to the attention of the team. Within the cylindrical scaffold, there was likely to be hollow space between the seeded microthreads and the encapsulating scaffold. This would increase the presence of bacterial microenvironments. Also, as previously mentioned, the funneled ends cause complications in fabrication and catheter delivery.

4.3 Scaffold Material Analysis

The encapsulating scaffold material incorporated into the AV node bypass mechanism must be composed of a non-degradable material. After the implantation and eventual degradation of the seeded fibrin microthreads, the cells composing the bypass mechanism must remain encapsulated by the outer scaffold. If the necessary amount of viable cells is not sustained locally within the heart, the device would not be able to propagate an electrical signal and would not complete its crucial function. The porous scaffold must not allow cells to migrate out of the device and wander into other areas of the heart. Not only would the AV node bypass mechanism

be dysfunctional, but also the migrating hMSCs could cause potentially harmful effects throughout the heart.

Prior to scaffold fabrication, the team conducted a thorough investigation of a range of materials. The scaffold material utilized must be biocompatible and minimize cells loss. The ideal scaffold material must be able to insulate the electrical current as it is passed from the SA node, through the device, bundle of His, and into the ventricles while minimizing the loss of current. To encapsulate the cells, the scaffold material must be non-degradable, insulatory, porous, flexible, and bioinert. The mechanical properties of the material were important to consider, as the scaffold must possess a high degree of elasticity, a high toughness and durability, and a low stiffness to withstand the contractile forces and cyclic loading of the heart. Based on these criteria, three materials were researched in depth for the application of an encapsulating scaffold: polyurethane (PU), polyethylene terephthalate (PET), and polytetrafluoroethylene (PTFE). Table 4 displays a summary of material properties of these three materials analyzed in a previous Major Qualifying Project completed at Worcester Polytechnic Institute in 2009. In addition, a proprietary material, 'Poly-X', had the potential to act as an insulator scaffold.

4.3.1 Polyurethane

Polyurethane is a thermoplastic, which is commonly utilized for its excellent mechanical properties and biocompatibility [59]. This material is known to demonstrate high toughness and durability similar to that of metal, while still possessing a high degree of elasticity [60]. Non-aromatic polyurethanes are known to have stronger adhesive properties and increased flexibility compared to aromatic polyurethanes [61]. Research has shown that polyurethane performs best under uniaxial tensile loading [61]. Polyurethane has a segmented block co-polymeric structure composed of diisocyanate, a chain extender and macrodiol (or polyol) [59]. Reaction of the three

primary materials results in the formation of linear segmented copolymers. The physicochemical properties of polyurethane can be modified by altering the ratio of hard segments to soft segments contained within copolymers [59]. The physical properties, as well as the blood and tissue compatibility can also be easily altered [59]. While polyurethane is classified as a non-degradable material, it is susceptible to oxidative, enzymatic, and hydrolytic degradation *in vivo* [59]. Non-thermal degradation of some polyurethane products may begin as low as 150 °C (300°F) to 180°C [62]. A variety of chemical modifications, such as crosslinking the materials with multi-functionalized natural compounds, can improve the biodegradability and biocompatibility of the material [60]. Chemically altered polyurethane can exhibit a degradation range between weeks and years [59]. Some of the biomedical applications of polyurethane include pacemaker leads, catheters, prosthetic valve leaflets, and coating materials for breast implants [59].

4.3.2 Polyethylene Terephthalate

Polyethylene Terephthalate (PET) is an essential technical plastic utilized as an engineering material within small, high-performance parts [63], [64]. While most often found as a semi-crystalline polymer, PET can undergo heat treatment during production to alter its percentage of crystallinity [64]. PET exhibits a low corrosion resistance and the widest temperature range of any polymer [64]. A unique property of PET is that its coefficient of friction is among the lowest of all materials [64]. Wear reducing compounds can also be sintered with PET to decrease the coefficient of sliding friction even further [64]. PET also exhibits the highest resistivity amongst a wide range of materials, possessing a very high dielectric strength and low dielectric loss. The material properties of PET make it a common material for applications such as plastic containers to hold food, beverages, cosmetics products, and

pharmaceutical products [63].

4.3.2 Polytetrafluoroethylene

Polytetrafluoroethylene, also known as Teflon, is a porous monofilament plastic polymer [65]. PTFE exhibits a high degree of flexibility and durability, as well as a high breaking strength [65]. While being negatively charged and permeable to many biomolecules and gases, polytetrafluoroethylene has the ability to simulate the thin layer of cells lining the inner surface of blood vessels, known as the endothelium [65]. This specific ability makes PTFE ideal in applications such as synthetic conduit materials for vascular bypass to treat heart disease and replacement of pericardium after cardiac surgical procedures [65].

4.3.3 'Poly-X'

Currently 'Poly-X' is being utilized in hollow fiber tubules at the University of Bath, England. Mechanical properties of 'Poly-X' remain unknown to the team. However, after meeting with the researcher from the University of Bath, the team was informed of the material's potential in the application of an AV nodal bypass mechanism. 'Poly-X' is a non-cell adhesive polymer that is biocompatible when implanted *in vivo*. Thus, 'Poly-X' remains a viable option as an insulator scaffold.

Moving forward, a PU/PET blend utilized for its combined properties and 'Poly-X' were assessed for design feasibility.

Table 4: "Summary of Candidate Material Properties" [66]

	PET	ePTFE	PU (ChronoFlex® C)
Biocompatible	Yes	Yes	Yes
Cytotoxic	No	No	No
Elastic Modulus	40-60*10 ⁴ psi	5.8-8.01*10 ⁴ psi	0.775-1.9*10 ⁴ psi
UTS	7.01-10.5 ksi	2.9-4.35 ksi	5.5-7.5 ksi
Yield Strength (Elastic Limit)	8.19-9.04 ksi	2.18-3.63 ksi	N/A
Multiaxial Fatigue	2.8-4.2 ksi (at 10 ⁷ cycles)	0.834-1.02 ksi (at 10 ⁷ cycles)	N/A
Shear Modulus	0.144-0.216*10 ⁶ psi	0.02-0.0276*10 ⁶ psi	N/A

4.4 Feasibility Analysis

The feasibility of each design aspect of the AV nodal bridge must be assessed prior to the development of a final prototype. The feasibility study was used to analyze the conceptual and preliminary designs in order to develop final design alternatives. Various tests on cell viability and cell migration were then performed on the final designs to determine the optimal design for the final prototype of the AV bridge.

4.4.1 Delivery Feasibility

The team decided to use a method of catheter implantation as a minimally invasive method to insert the device into the heart. The specific catheter the team planned to use was the catheter discussed in *Chapter 2* developed by a 2011 Major Qualifying Project team. The method of device implantation using this catheter presented a number of constraints to consider in the development of the AV node bypass mechanism.

Protection of the scaffold, thread, and cellular components of the device must be ensured to result in effective device implantation and function. Without safe and secure insertion through a catheter device, the necessary amount of viable cells would not be delivered into the heart and the signal would not be propagated into the right ventricle, compromising the function of the

device. The method of implantation influenced the size, shape and material composition of the device to guarantee that the device could fit in the catheter. Specifically, the current design of the catheter only accommodates for materials of maximum 1.0 mm in diameter. The team needed to consider the flexibility of the material and the forces experienced by the device, specifically if it would be in tension or compression during implantation throughout catheter insertion. If the AV node bypass mechanism is not designed with the proper mechanical properties, the device could experience mechanical failure before complete implantation.

Through discussion with one of the students of the catheter Major Qualifying Project team, it was confirmed that these constraints could be overcome for the bridge design. The student believes the catheter design could be slightly altered to accommodate for the AV nodal bypass bridge. This confirms the feasibility of the use of catheter implantation for the final design.

4.4.2 Structure

The first design aspect that was evaluated for feasibility was the structure of the AV bridge, specifically the insulating scaffold. After further discussion with the client, it was decided that the cylinder formation of the preliminary designs was ideal due to its ease of catheter implantation. The cylindrical scaffold would be flattened when implanted into the heart due to the contractile and cyclic forces it will experience as stated by the client. The flattening of the cylindrical scaffold will decrease the likelihood of bacterial growing in microenvironments within the device.

After deciding upon a cylindrical scaffold, the plain bundle and funnel cylindrical scaffolds were assessed for feasibility. The funnel scaffold presents limitations to the fabrication methods utilized, such as electrospinning. Different fabrication techniques would be needed to

create the straight cylindrical shape and the funneled ends. In addition, the diameter of the funneled ends would significantly impact the catheter delivery method, and thus the diameter of the straight section. The outer diameter of the funneled ends must not be greater than 1mm, the inner diameter of the specialized catheter. Therefore, the outer diameter of the straight section must be decreased. This may present further limitations loading the scaffold with threads seeded with hMSCs. Due to these limitations, the final design will be based upon the plain, cylindrical bundle.

4.4.3 Fabrication Methods

After assessing structure of the scaffold, the feasibility of various fabrication methods were assessed. Fabrication methods under consideration were laser micro-etching, electrospinning, and solvent casting and particulate leaching.

4.4.3.1 Laser Micro-etching

Upon initial analysis, working with a collaborative team in Lithuania to produce a laser micro-etched scaffold seemed feasible. The laser micro-etching fabrication method allows for consistently produced and controlled pore sizes. Pore control would allow for large pore sizes on the ends of the scaffold to promote gap junction formation and smaller pore sizes along the center of the scaffold to allow for nutrient passage as well as prevent cell migration. This method would allow for variations in pore sizes to be feasible without altering the thickness throughout the scaffold. However, with time as a major project constraint, it was determined that it was not feasible to ensure that the scaffold is fabricated and shipped with enough time to perform cell viability tests and collect data for the final project presentation in April 2015.

4.4.3.2 Electrospinning

The second fabrication method assessed for feasibility was electrospinning. Electrospinning is a common fabrication method used to produce porous scaffolds. A previous

Major Qualifying Project completed at Worcester Polytechnic Institute in 2012, successfully produced an electrospun scaffold made of a PU/PET blend [67]. However, one limitation of electrospinning is limited pore size control and consistency. Thus, it is difficult to produce the desired pore sizes uniformly along the entirety of the scaffold. After speaking with BioSurfaces Inc., an electrospinning company based out of Auburn, MA, a method of attempting to control this pore size was developed. The company provided the knowledge of the correlation between the thickness of the scaffold and the pore sizes produced through electrospinning. The thicker the scaffold, the smaller the pore sizes, and vice versa. There is no direct way to control the pore sizes produced through electrospinning, however, the thickness of the scaffold can be controlled.

BioSurfaces developed a method of producing an electrospun cylindrical scaffold to our specifications. After spinning a cylindrical mandrel to attempt to produce the thickness for 2.0-2.5 μm pore sizes that were necessary for gap junction formation, the center of the mandrel could be spun again to produce smaller pore sizes. However, this impacted the thickness of the center of the tube and may have decreased the area in which the threads must be inserted, in addition to restricting catheter loading. The team decided the feasibility of this fabrication method should be further assessed through experimentation, as discussed in a later section.

4.4.3.3 Solvent Casting and Particulate Leaching

To assess the final fabrication method of solvent casting and particulate leaching, the team met and spoke with a researcher from the University of Bath in regards to the development of 'Poly X' hollow fiber tubules through this fabrication method. The team planned to further assess this material and pore size feasibility in regards to this method during a future correspondence with the University of Bath.

4.4.3.3.1 Material Analysis

Upon previous material analysis, it was determined that the scaffold would be composed of PU/PET utilized for its combined properties. However, after speaking with the researcher of the University of Bath, the team was informed that hollow fiber tubules have not been produced with a PU/PET blend in the past. Currently, the tubules are composed of a proprietary polymer, 'Poly-X' which is non-degradable and non-cell adhesive. The team decided to look into possible solvents that could be utilized in order to create a PU/PET hollow fiber tubule. For this to be possible, one solvent must dissolve PU and PET while the other solvent must not. In addition, both solvents must be miscible for a successful tubule to be fabricated.

Throughout discussion, it was determined that 'Poly-X' was a potential material that could be utilized in the AV bridge. Specifically, a scaffold consisting of 'Poly-X' in the center would prevent hMSCs from adhering to the scaffold and potentially forming gap junctions through the pores. Thus, the cell-adhesive PU/PET blend could be sealed onto the ends of the 'Poly-X' scaffold to promote gap junction formation. In the event that producing a PU/PET hollow fiber tubule was not plausible, electrospinning PU/PET ends of the scaffold remained a feasible option despite uncontrollable pore sizes. These ideas are presented in the following section, *Decisions on Final Designs*. The feasibility of a complete PU/PET hollow fiber tubule and a 'Poly-X'/PU/PET tubule needed to be further assessed through analysis.

4.4.3.3.2 Pore Size Analysis

The feasibility of controlled pore size is another design aspect that was evaluated. Solvent casting and particulate leaching offers more control over pore size compared to electrospinning. The preliminary scaffold designs consist of two different pore sizes, $\leq 0.4\mu\text{m}$ in the center to promote the nutrient diffusion and inhibit cell migration and $2\text{-}2.5\mu\text{m}$ on the ends to promote gap junction formation between hMSCs and native cardiomyocytes. After speaking with the

University of Bath, the researcher informed the team that the smallest pore size produced through the method of solvent casting and particulate leaching was 2.0 μm . Upon further analysis, a tube of consistent pore size (2.0 μm) and thicker inner diameter of the center of the scaffold may still be able to prevent cell migration and prevent gap junction formation along the middle of the tube. Utilizing ‘Poly-X’ as a non-cell adhesive material in the center of the tubule also remained a feasible option. However, the feasibility of sealing thinner PU/PET ends to the center of the scaffold must be addressed. Further analysis of using a uniform pore size, varying scaffold thickness, and utilizing ‘Poly-X’ needed to be completed.

4.4.4 Sealing Methods

Sealing ends of different pore size or material to the center of the scaffold is vital for gap junction formation, while prohibiting the migration of the cells out of the ends of the scaffold. However, sealing methods must not affect cell viability or structural integrity of the scaffold. Two sealing methods were investigated: heat sealing and BioGlue®.

4.4.4.1 Heat Sealing

Heat sealing is a sealing method that has been utilized in previous Major Qualifying Projects at WPI. However, the use of heat to seal a small diameter scaffold required complete control and precision. Sealing the ends of the scaffold would occur once the threads seeded with hMSCs are inserted into the scaffold. Using heat to seal the ends prevents a harmful risk to the viability of cells and structural integrity of the scaffold. Due to the importance of cell viability, heat sealing too close to the microthreads was deemed a risk. However, this method was still tested on the scaffolds, as discussed in a later section.

4.4.4.2 BioGlue®

In order to seal the ends of the scaffold, the use of BioGlue® was considered as an option. BioGlue® reduces the risk of scaffold denaturation due to heat and potentially presents a

lesser risk of cell death in comparison to heat sealing. Micro-forceps can be used to secure the scaffold and apply to BioGlue® to a controlled area. The overall feasibility of using BioGlue® to seal a small diameter tubule needed to be assessed further through experimentation. However, due to time constraints and availability of the product, the team was unable to obtain the product to perform testing with. Therefore, heat sealing was the primary method of sealing analyzed as discussed in later sections.

4.4.5 HCN Transfected Cell Availability

In terms of the functional AV nodal bypass mechanism, assessment of the function of the bridge to pass current along the length of the bridge with minimum current drop between the atrium and the ventricle was inhibited. The availability of HCN transfected hMSCs was a large factor, as these cells are needed along the length of the bridge to fire action potentials in the case of current loss in the radial direction. Professor Gaudette stated that the ability to obtain these cells for this project was highly unlikely. Also, the cost of HCN transfected cells may have exceeded our budget constraint. As an alternative, non-transfected hMSCs in addition to neonatal rat cardiomyocytes were utilized. Therefore, it was not feasible to test the full functionality of the final prototype within the budget and time constraints.

4.5 Decisions on Designs

Taking the preliminary designs and the concerns with each into consideration with the various methods of fabrication, the team narrowed potential designs down to three viable options. The designs make use of the hollow fibers from the University of Bath in England and electrospinning methods of fabrication, as mentioned above in the feasibility study.

4.5.1 Option 1: 'Poly-X' and PU/PET Hollow Tubes

The first option developed by the team was a scaffold with the center portion consisting of a ‘Poly-X’ hollow tube and two ends made of PU/PET hollow tubes as shown in Figure 19. The two portions of the scaffold would be fabricated separately and glued or heat sealed together. The entire scaffold would ideally have pore sizes of approximately 2-2.5 μm . This pore size on the ends of the scaffold would allow for the gap junction formation between the native cardiomyocytes and the hMSCs within the encapsulating scaffold. The center ‘Poly-X’ portion would have this pore size, but be thicker than the ends to prevent gap junction formation, as it was necessary to minimize current loss throughout the bridge. The ends of this scaffold would be sealed to prevent cell loss, as discussed above in the preliminary design section.

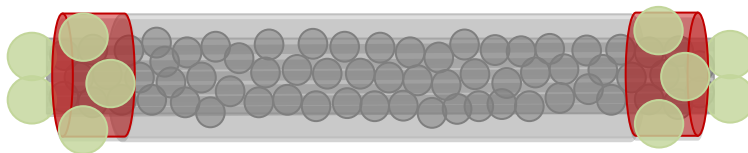


Figure 19: Design Option 1: Red is the PU/PET Hollow Tubes; Grey is the Poly-X Hollow Tube Scaffold.

The major limitation in regards to this design was the availability of a solvent and non-solvent that correlates with the PU/PET substance to allow for the fabrication of the hollow tubes. If this information could not be obtained, or is nonexistent, this design would not be viable.

4.5.2 Option 2: ‘Poly-X’ Hollow Tube and PU/PET Electrospinning

The second option for the design the team developed is shown below in Figure 20. The center portion would be made of a ‘Poly-X’ hollow tube, while the ends would be made of a PU/PET electrospun material. These two portions would be sealed together to create the entire scaffold. Again, the pore size of the entire scaffold would be approximately between 2-2.5 μm

with the center portion having a greater wall thickness to prevent gap junction formation. Again, the ends would be sealed to prevent cell migration from the scaffold.

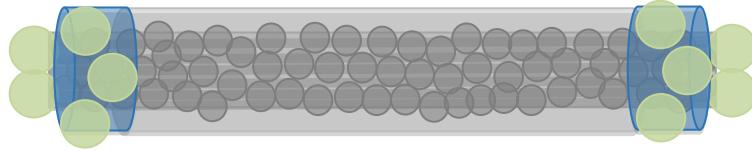


Figure 20: Design Option 2: Blue is the PU/PET Electropun Scaffolds; Grey is the 'Poly-X' Hollow Tube Scaffold.

4.5.3 Option 3: PU/PET Electrospinning

The third and final option developed by the team is a complete PU/PET electrospun scaffold as shown in Figure 21. This would be an option if the hollow tubes were deemed unfeasible or unavailable. The center portion of the PU/PET scaffold would ideally have smaller pore sizes of about $\leq 0.4 \mu\text{m}$ to allow for the nutrients to enter the device, but prevent the cells from migrating or forming gap junctions. This portion would naturally be thicker due to the pore size of electrospun materials being proportional to the thickness of the material. The ends of this scaffold design would ideally have pores of size 2-2.5 μm to allow for the gap junction formation. Again, the ends of the scaffold should be sealed to prevent migration of the hMSCs.

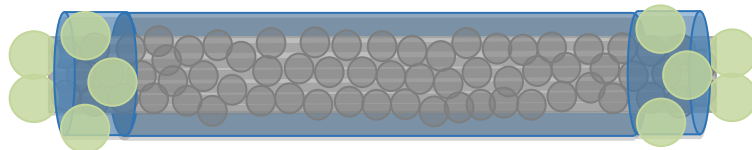


Figure 21: Design Option 3: Blue is the PU/PET Electrospun Scaffold

4.5.4 Design Specifications

A number of specifications were confirmed for the design as shown below in Table 5.

Table 5: Ideal Design Specifications

Scaffold	Pore Size of Hollow Tubes = 2-2.5 μm	Pore Sizes of Electrospun Scaffolds = 2-2.5 μm and $\leq 0.4 \mu\text{m}$	Wall Thickness for Gap Junction Formation = 10-20 μm [68]	Wall Thickness for Hollow Tubes = $> 90 \mu\text{m}$ [68]	Length of Ends of Scaffolds = 0.4 cm
Fibrin Microthreads	Bundle Size = 6 or 12 threads				
hMSCs	100,000 seeded				
Entire Design	Length = $\geq 2 \text{ cm}$	Outer Diameter = 1 mm [57]			

As mentioned above in the feasibility study, the pore size of the hollow tubes could not be made as small as the desired $\leq 0.4 \mu\text{m}$. However, the pore size could still remain at a size of 2-2.5 μm if the thickness of the center of the device was increased. The wall thickness of the ends of the scaffold where gap junctions form should be 10-20 μm , as calculated in previous MQP work to be ideal for gap junction formation [68]. The thickness of the ‘Poly-X’ center portion tubes would be $> 90\mu\text{m}$ [68] as this number has been shown to prevent migration of hMSCs. The length of the caps, or ends, of the scaffolds would be about 0.4 cm on each end of the scaffold if it were to be 2 cm long, allowing for the center portion of the scaffold to be a minimum of 1.2 cm in length. The client suggested to begin testing with a 6 or 12 thread bundle of fibrin microthreads and seeded with 100,000 hMSCs. In studies conducted in the client’s lab at WPI, the 12 thread bundle had been shown not to inhibit cardiomyocyte contraction and promote passage of current. Overall, the entirety of the design would have a minimum length of 2 cm and an outer diameter of 1-2 mm [57].

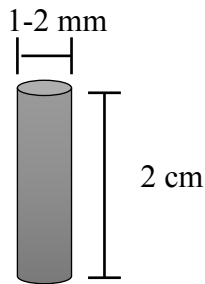
4.5.5 Design Calculations

4.5.5.1 Surface Area of Cylindrical Bridge

$$A = \pi * d * L$$

$$A = \pi * (1\text{mm}) * (20\text{mm})$$

$$A = 62.83 \text{ mm}^2$$



4.5.5.2 Forces Exerted by the Heart

The human heart exerts average blood pressures of 120 mmHg in systole (contraction) and 80 mmHg diastole (relaxation). These pressures can be converted into forces exerted by the heart, which will therefore also be exerted on the AV bridge. The equations below determine the mechanical strength the scaffold will need to withstand in the case of the length of the bridge being the minimum of 2 cm with a diameter of 1 mm.

$$P_{heart} = \frac{F_{heart}}{A_{bridge}}$$

$$F_{heart} = P_{heart} * A_{bridge}$$

$$\text{Diastole} \rightarrow 80 \text{ mmHg} = 0.01066576 \frac{\text{N}}{\text{mm}^2}$$

$$F_{diastole} = P_{heart} * A_{bridge}$$

$$F_{diastole} = 0.01066576 \frac{N}{mm^2} * 62.83 mm^2$$

$$F_{diastole} = \mathbf{0.6698 N}$$

$$Systole \rightarrow 120 mmHg = 0.01599864 \frac{N}{mm^2}$$

$$F_{systole} = P_{heart} * A_{bridge}$$

$$F_{diastole} = 0.01599864 \frac{N}{mm^2} * 62.83 mm^2$$

$$F_{diastole} = \mathbf{1.0045 N}$$

4.6 Feasibility Testing

In testing the feasibility of the design, the team moved forward with the electrospinning fabrication method as the availability of the hollow tubules was deemed unfeasible. Various samples of electrospun PU/PET scaffold were obtained at 20, 40, and 50 μm . The feasibility of the design was evaluated based on scaffold thickness in relation to pore size.

4.6.1 Sealing and Thread Insertion Methods

In terms of the methods of sealing the ends of the encapsulating scaffold, heat sealing and needed to be tested accordingly in order to confirm the use of the method of sealing for use in the AV bridge. Experiments were performed in non-sterile environments with the PU/PET scaffolds of any size thickness.

For heat sealing, the scaffold material was tested using a soldering tip, hereon described as a fine-tip heat source. The fine-tip heat source was controlled in terms of temperature to

assure the heat applied would shrink the material, while not degrading the material. The fine-tip heat source was applied to the scaffold and also held at a distance from the scaffold so 500-600°F, as both heat sources were likely to melt the scaffold. The resulting sealed scaffold samples were observed and imaged using microscopy in order to visually confirm that the method sealed the scaffold.

During the first set of experiments, the scaffolds were tested without any cells seeded on the materials. This ensured that the heat sealing was working properly before involving the use of cells, and that the heat does not cause excessive damage to the scaffold. After the heat sealing was deemed possible and did not harm the material too much, the overall AV nodal bypass device was assembled. 45,000 hMSCs seeded on a 6X suture of fibrin microthreads were encapsulated in a cylindrical scaffold sample. The ends of the scaffold with the seeded threads inside were then sealed using the fine-tip heat source. This test allowed the determination of the cell viability after heat sealing.

Finally, after heat sealing was confirmed as a viable method of sealing, decisions on where the scaffold would be sealed were concluded. The team brainstormed three possible methods of how the seeded fibrin microthreads can be inserted into the encapsulating scaffold, which all involve the need for sealing in different places of the scaffold. Figure 22 through Figure 24 show the options that were considered in order to determine the optimal method of inserting threads into the encapsulating scaffold.

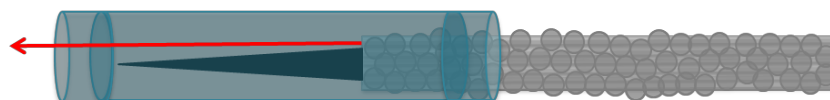


Figure 22: Thread Insertion Option 1

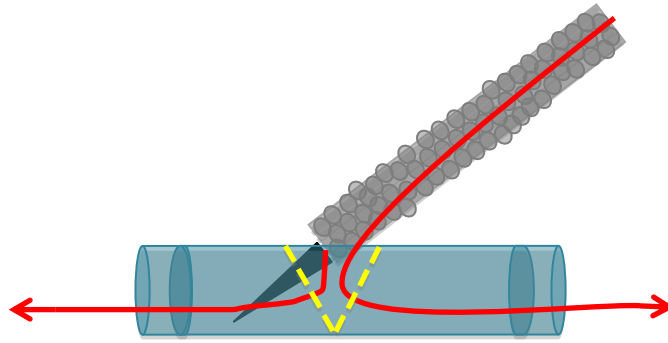


Figure 23: Thread Insertion Option 2

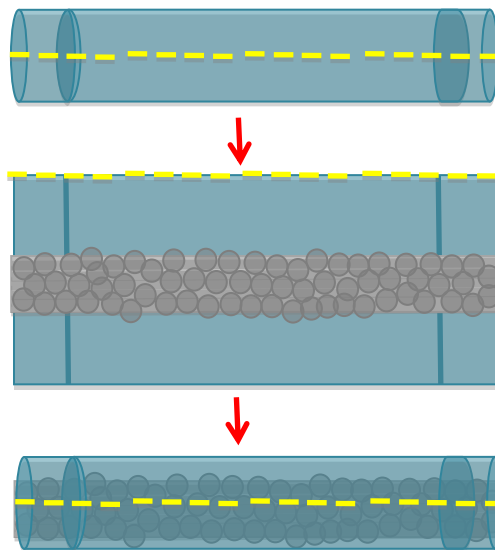


Figure 24: Thread Insertion Option 3

Figure 22 shows the seeded threads simply being pulled through the cylindrical scaffold with a straight needle. In this option, the ends of the cylindrical scaffolds would be the only area that needed to be sealed. Figure 23 shows the scaffold being cut in the center across the yellow dotted lines where the seeded threads can be inserted into the scaffold one end at a time. In this option, the scaffold would need to be sealed at the cut center, as well as at the ends of the cylindrical scaffold. Figure 24 shows the tubular scaffold being cut across its length to allow the tube to be opened for insertion of the seeded threads. This option called for the cut length across

the scaffold to be sealed, as well as the ends of the tube. Through discussion the team determined that option was the most feasible in terms of minimizing sealed surface area and maintaining cell viability.

4.6.2 Cell Viability

It is important that the scaffold material used did not harm the cells. To determine if the PU/PET scaffold was biocompatible, LIVE/DEAD staining was performed. According to the procedure in Appendix III, this test utilizes Hoechst dye, ethidium homodimer, and calcein AM to determine the cell viability of the samples. Hoechst dye is a fluorescent dye that stains the DNA of live and fixed cells. Ethidium homodimer is a fluorescent dye that is unable to pass through the membrane of living cells. When cells are dead, the membrane is disrupted allowing for the ethidium homodimer to enter the cell and stain the DNA in the nucleus. Calcein AM is a fluorescent dye that has the ability to pass through the cell membrane of a living cell. This dye enters the living cell and fluoresces the cell cytoplasm. Therefore, living cells are stained with one fluorescent dye, dead cells are stained with a separate fluorescent dye, and all nuclei are fluoresced during the same procedure. In terms of the AV bridge, LIVE/DEAD staining was primarily performed on PU/PET scaffold samples of 20, 40, and 50 μ m thick seeded with approximately 40,000 hMSCs in order to determine the toxicity of this material in terms of cell viability.

4.6.3 Migration

In order to determine if the encapsulating scaffold successfully prohibits the migration of cells from the AV bridge, Hoechst and Phalloidin staining was performed. As stated above, Hoechst is a fluorescent stain that binds to the nuclei of cells, while Phalloidin is a chemical that binds to the F-Actin in the cells. According to the procedure found in Appendix IV, approximately 80,000 hMSCs were seeded on one side of the scaffold using the Gaudette-Pins

transwell as shown in Figure 25 and incubated for 4 days. Following the incubation period, the cells were fixed and stained with Hoechst and Phalloidin to visualize the location of the cells. Both sides of the scaffold were imaged using fluorescent microscopy in order to determine if any cells migrated through the pores. This test was performed on scaffolds with thicknesses of 20 μm , 40 μm and 50 μm in order to determine the optimal thickness to prevent migration.



Figure 25: Gaudette-Pins Well

Chapter 5: Design Verification Results

5.1 LIVE/DEAD Staining

Initially, it was vital to ensure the PU/PET scaffold material was biocompatible and did not harm the cells. A number of samples of the scaffold at thickness of 20 μm , 40 μm and 50 μm were seeded with hMSCs and were incubated for four days. Following this incubation period, the scaffolds with hMSCs were stained with blue Hoechst, green calcein AM, and red ethidium homodimer dyes and then imaged through the use of fluorescent microscopy. Images obtained at 10x are shown in Figures 26 and 27 below and were utilized for calculations of the cell viability.

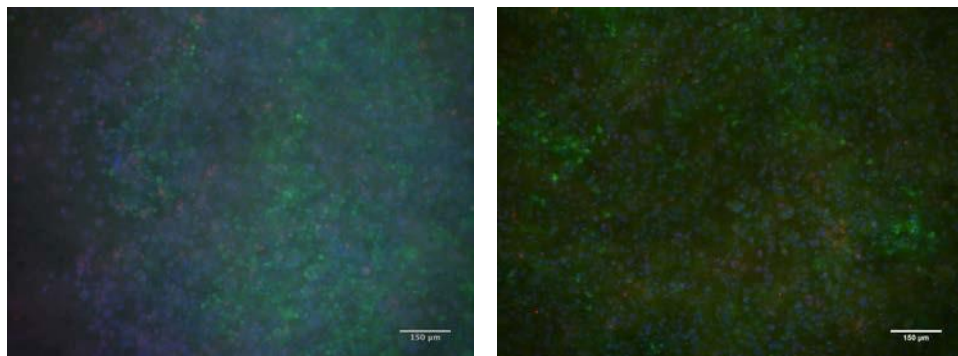


Figure 26: Samples 1 & 2: 20 μm scaffolds with a 96.3% cell viability (left) and a 98.2% cell viability (right) with the scale bar representing 150 μm

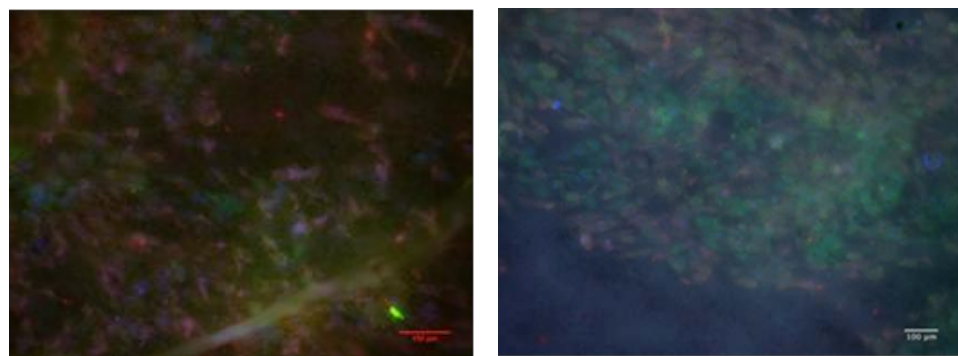


Figure 27: Samples 3 & 4: 40 μm scaffolds with a 97.2% cell viability (left) and a 98.6% viability (right) with the scale bar representing 100 μm

ImageJ software was used to count the total number of nuclei, the number of living cells, and the number of dead cells, as shown in Table 6 below for the samples shown in the figures above. A ratio of living cells to total cells was calculated and an average of $97.8 \pm 1.03\%$ cell viability was determined.

Table 6: Results of LIVE/DEAD staining on four scaffold samples

	Nucleus Count	Dead Cell Count	Viable Cells
Sample 1 (20 μm)	216	3	98.2
Sample 2 (20 μm)	200	7	96.3
Sample 3 (40 μm)	99	1	98.6
Sample 4 (40 μm)	77	2	97.2

5.3 Cell Migration

Cell migration testing was performed to determine the ideal thickness of the scaffold to prevent cells from wandering outside of the device. Cells were seeded onto one side of 20 μm , 40 μm , and 50 μm scaffolds and allowed to incubate for four days. Following the incubation period, the cells were stained with Hoechst and Phalloidin dyes in order to visualize the cells through fluorescent microscopy, shown Figures 28-30 below. It was determined that the 20 μm thickness was too thin and allowed for cell migration through the scaffold material, whereas the 40 μm and 50 μm samples prevented cell migration as the images in Figures 29 and 30 only shown the auto fluorescence of the scaffolds in the images obtained of the bottom of the scaffolds.

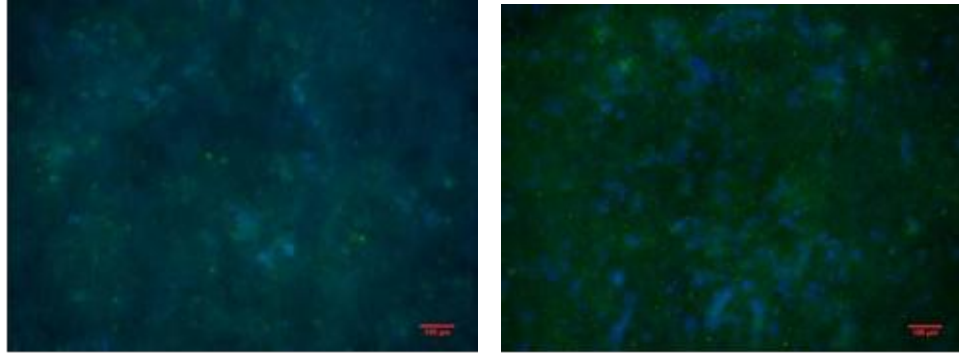


Figure 28: Hoechst and Phalloidin on top (left) and bottom (right) of 20 μ m scaffold with the scale bar representing 100 μ m

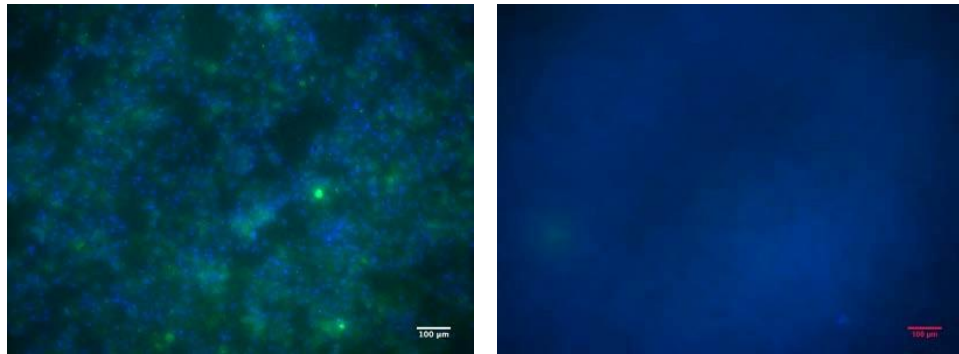


Figure 29: Hoechst and Phalloidin staining of top (left) and bottom (right) of the 40 μ m scaffold with the scale bar representing 100 μ m

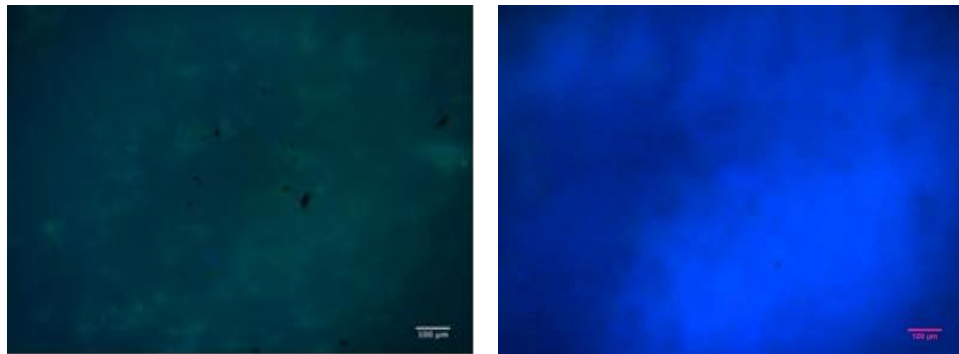


Figure 30: Hoechst and Phalloidin staining on top (left) and bottom (right) of the 50 μ m scaffold with the scale bars representing 100 μ m

5.3 Heat Sealing

As previously mentioned, the ends of the scaffold were clamped together using forceps and a fine tip heat source was applied to each end. The PU/PET scaffold was then imaged using high magnification microscopy as shown in Figure 31 below.

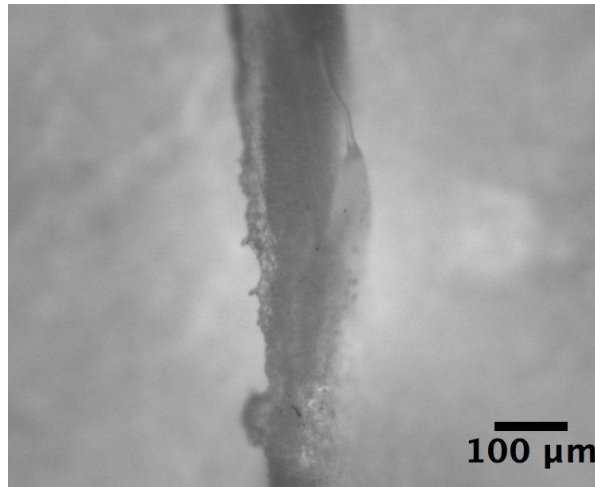


Figure 31: Seal of scaffold sample displayed in the center of the PU/PET scaffold

To ensure the heat sealing did not negatively harm the cells, LIVE/DEAD staining was then performed on the sealed scaffold. 45,000 hMSCs were seeded onto fibrin microthreads and were stained utilizing blue Hoechst dye, red ethidium homodimer, and green calcein AM following the extraction of the thread from the sealed scaffold after the fine-tip heat source was applied. The cells were then imaged utilizing fluorescent microscopy as see in Figure 32 below.

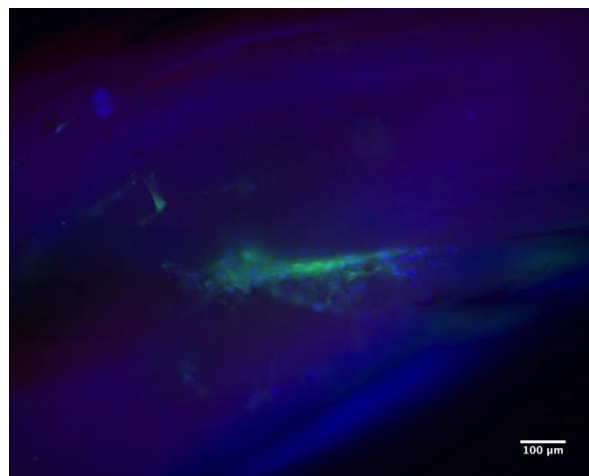


Figure 32: LIVE/DEAD staining of hMSCs on fibrin microthreads immediately after heat sealing 50 μm PU/PET scaffold

The blue circles in the above image represent cell nuclei. Living cells can be seen where there is green surrounding the blue nuclei, whereas dead cells can be seen where there is red concentrated inside of the blue nuclei.

Chapter 6: Discussion

This project began the initial development of an AV nodal bypass device through the production of an encapsulating PU/PET electrospun scaffold. The project's focus on the encapsulating scaffold allowed for the addressing of a number of the main functions desired for the final AV bridge device. The collecting, passing and delivering of current from the atrium to the ventricle with minimal loss of the current along the length of the bridge, as well as the minimal loss of the cells within the device, were both accounted for through the development of the encapsulating scaffold.

6.1 LIVE/DEAD Staining Results

Biocompatibility of the overall device is ranked as the third most important objective according to both the team and the client as discussed in *Section 3.2*. The device must not be cytotoxic to the patient or the hMSCs used within the device. In order to test for the biocompatibility of the scaffold, the team performed LIVE/DEAD staining on hMSCs seeded onto the scaffold samples in order to determine if the scaffold would be cytotoxic to this specific cell type. The results shown in *Section 5.1* verify the biocompatibility of the PU/PET material for its use as the encapsulating scaffold for the AV node bypass device.

A sample of four scaffolds seeded with hMSCs that underwent the LIVE/DEAD staining were analyzed with ImageJ software in order to determine the ratio of viable cells to dead cells found on the scaffold. Cell nuclei stained with Hoechst dye were counted on the representative images with the ImageJ software, while the dead cells within the images were counted manually. Cells were characterized as dead when the red ethidium homodimer dye aligned with the blue Hoechst dye within the nucleus of a cell. Through this method of counting, it was determined

that the average cell viability on the scaffold samples was approximately $97.8 \pm 1.03\%$ by taking the average viability percentages of each of the four samples shown in Table 6. These calculations numerically verify the biocompatibility of the scaffolds.

6.2 Migration Study Results

As mentioned above, the migration of cells is an undesirable characteristic of the AV node bypass device. The loss of cells via migration through the scaffold pores needed to be controlled for the device to function as desired. Therefore, migration testing was performed on the three different thicknesses of the scaffold: 20 μm , 40 μm and 50 μm . The results of these tests presented in *Section 5.2* show that the 40 μm and 50 μm samples were preferable for the use in the device, as they successfully prevented the migration of the hMSCs from the top of the scaffold to the bottom of the scaffold over an incubation period of 4 days. However, as shown in Figure 28, the 20 μm scaffold sample was unable to prevent the migration of the cells as a large number of hMSCs were seen on the bottom of the scaffold after the 4 day incubation period. Therefore, these results allowed for the team to conclude that the use of the 20 μm scaffold thickness is unwarranted for the AV node bypass device. These results also support the recommendation of the use of a PU/PET scaffold for the final device that has a thickness in all sections of the device greater than or equal to 40-50 μm , as migration of cells needs to be contained throughout the entire device.

6.3 Heat Sealing Results

Based on the desired functions of the device, cell loss and migration would be detrimental to the overall function of the AV node bypass device. With the loss or migration of cells from inside the encapsulating scaffold to the external environment of the heart, there may be an inability for gap junctions to form between all hMSCs along the length of the bridge, in turn inhibiting the passage of current from the atrium to the ventricle. Without enough cells in

the device, the main function of collecting, passing and delivering the current from the atrium to the ventricle would not be able to be completed.

In order to prevent the loss of cells and migration of cells from the two ends of the final device, heat sealing testing was performed on cylindrical scaffold samples as described in *Section 5.3*. Observations made under an inverted microscope visually confirm that the scaffold samples were successfully sealed with the application of a fine tip heat source. There was no light that was able to shine through the scaffold samples at the sealed area, suggesting that the seal was complete. In addition, the results of the LIVE/DEAD staining of the sealed hMSC seeded fibrin microthreads located inside of the scaffold sealed with the fine tip heat source suggest that the heat source did not negatively affect the cells. These results verify the use of a fine-tip heat source as the method of sealing the ends of the cylindrical scaffold to prevent cell loss and migration from the device.

6.4 Limitations in Design Verification

There are a number of limitations in the verification of the device that the team encountered. First and foremost, the variation and amount of different scaffold thickness samples was a limitation in the project. The availability of resources to develop more samples with different thicknesses hindered the characterizing of appropriate thickness of the encapsulating scaffold. In terms of the cell viability calculations, the sample size of four scaffold images used does not provide statistically relevant results, as the sample size is much too small. The team was only able to perform two LIVE/DEAD staining procedures, which provided a number of 10x and 5x images for use. However, the 5x images were unable to be processed with the ImageJ software to count the cell nuclei in the images, leaving a smaller amount of 10x images to analyze. Further, the use of the fine-tip heat source was not a controlled method of sealing the

device. There is room for improvement in the process of sealing the device, as the process should be controlled producing uniform results each time of application. Additionally, the Hoechst and Phalloidin staining for migration was only performed once on one sample of each thickness due to the time constraints of the project and limited availability of Gaudette-Pins wells.

Furthermore, the lack of availability of cardiomyocytes in the lab prohibited the team from both verifying the thickness needed for gap junction formation and verifying the passage of current through the bridge. These tests will be recommended for future groups to perform and will be discussed further in *Chapter 8*.

6.5 Device Impacts

In terms of the economic impact of the device, the comparison of the cost of electrical cardiac pacemakers and the AV node bypass device should be considered. The average electrical cardiac pacemaker currently costs \$35-45,000 [5], [6]. Based on data provided from the Professor Gaudette's lab and Biosurfaces, Inc., the overall estimated price of developing the AV node bypass device would be about \$1,500 as shown in Table 7 below. It is important to understand that the aforementioned price of the electronic cardiac pacemaker includes the manufacturing costs, the sales force costs, and all other associated costs with developing, marketing and selling a product. The calculated cost of the AV node bypass device does not include these factors. The team believes the AV node bypass device would be competitive with the current pricing of pacemakers, but would ideally be cheaper. With the need for less material as the device is much smaller than an electrical cardiac pacemaker, it is assumed that the pricing of the device would be cheaper.

Table 7: Cost of components needed in development of AV node bypass device

AV Node Bypass Device	
hMSCs	\$717 (20 million cells)
Cell Culture Media	\$270 (2 bottles)
Trypsin	\$39 (1 bottle)
T-Flasks	\$50
Fibrin Microthreads	\$285 (420 threads)
Cylindrical Scaffold	\$145 (100 scaffolds)
Total:	\$1,506

Ideally, the device would influence society in a positive manner by providing an alternative to the current pacemaker. The device would overcome the disadvantages of the pacemaker and present society with a better, cheaper option for the treatment of AV nodal block. In terms of political ramifications, with this device hypothetically replacing the use of electrical cardiac pacemakers, many companies would be affected negatively. The device would ideally eliminate the need for the electronic pacemakers, therefore putting certain companies out of a product. This may cause negative political ramifications within the medical device industry.

By eliminating the use of the electrical cardiac pacemaker in the treatment of AV nodal block by making use of the AV node bypass device, there would not be a negative impact on the environment. Electrical cardiac pacemakers are larger than the AV node bypass device would be. Therefore, there would be a decline in the usage of materials for treatment of this disease. There is also no need for an outside power source for the AV node bypass device, which will eliminate the need for batteries. This will allow for the need to disposing of the batteries to decrease, which is better for the environment. Overall, the device would not affect the environment in a negative manner.

In terms of the ethics of the device, the team foresees no negative impact. The use of stem cells is often an ethical concern in society, however this concern often stems from the use of embryonic stem cells. These stem cells are obtained from embryos and are often the topics of much ethical controversy. However, human mesenchymal stem cells are obtained from adults. Therefore, this eliminates the potential negative ethical impact in society.

The finalized device, after further research and work, would not provide any health or safety risks. The PU/PET scaffold has been shown to be biocompatible and would not produce a cytotoxic effect in the body. The hMSCs would be contained by the encapsulating scaffold, which would prohibit the hMSCs from wandering from the device. Finally, the fibrin microthreads have also been shown to be biocompatible and would not produce cytotoxic effects once implanted in the body.

Finally, the manufacturability and sustainability of the final AV node bypass device needs to be considered. The manufacturing of the cylindrical scaffold consisting of a pattern of different thicknesses may possibly present challenges in the success of the device. Biosurfaces, Inc. expressed the challenge of developing such a small cylindrical scaffold through the electrospinning process. Additionally, a pattern of thick and thin regions may cause even greater challenges. In terms of the cell choice, the final device would make use of HCN2 channel transfected hMSCs. The availability of these cells and success rate of transfection may present challenges in terms of sustainability of the device.

Chapter 7: Final Design and Validations

Upon project analysis, the team developed the final design of the AV node bypass device as shown in Figure 33. This device was developed from the initial, straight-line conceptual design, due to diameter restrictions presented by the catheter method of implantation. The scaffold material used in the device is a PU/PET blend, utilized for its favorable mechanical properties. LIVE/DEAD staining performed on hMSCs seeded onto PU/PET scaffold samples confirmed the material's biocompatibility. The scaffold is electrospun at desired thicknesses in order to collect, transmit, and deliver current along the length of the seeded microthreads contained within the cylindrical scaffold. In terms of catheter implantation, the final design must be mechanically stable, as the catheter lead is inserted and snaked through the right, internal jugular vein into the right chambers of the heart. In addition, the final design accommodates for a fine-tip heat source to be applied to the ends of the scaffold without negatively impacting hMSC viability.

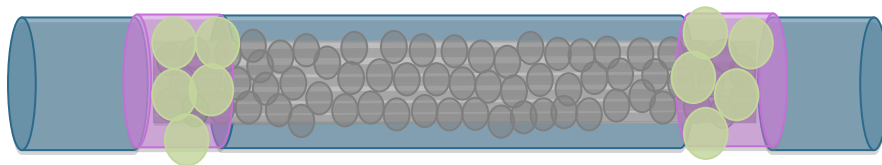


Figure 33: Final design with outer thick regions (blue), inner thin regions (pink) and a center thick region (blue) all at least 40-50 μm thick.

As seen in Figure 33, the final scaffold design consists of a thick, electrospun region of at least 40-50 μm in thickness in order to prevent cell migration. This thick, center region is composed of small pores that will prohibit cell migration and gap junction formation with native cardiomyocytes outside of the scaffold. Gap junctions between hMSCs seeded along this region

of fibrin microthreads are responsible for passing current along the length of the bridge. However, the absence of gap junctions with native cardiomyocytes along the center of the bridge allows for minimal current loss as it is transferred from the atrium to the ventricle. The electrospun center contains pores that are large enough to allow nutrients to reach the cells contained within this region of the scaffold.

The pink regions displayed in Figure 33, are composed of the same electrospun PU/PET material as the center region. However, these regions are thinner in order for the hMSCs to form gap junctions with native cardiomyocytes located within the heart. Although these regions of the scaffold are thinner than the center portion, the thickness must be at least 40-50 μm in order to contain cell migration. Based on the electrospinning fabrication method, the thinner regions of the scaffold contain larger pores compared to the center region, allowing for the cells on the end of the scaffold to form gap junctions with native cardiomyocytes. When placed within the central fibrous body of the heart, one thin region will be located in the right atrium, as gap junctions between native cardiomyocytes and seeded hMSCs are needed to collect the electrical current produced by the SA node. This second thin region will be located in the ventricle to deliver the current through the gap junctions formed between hMSCs and cardiomyocytes located in the ventricle.

The outer ends of the scaffold are thick, PU/PET material utilized for sealing and mechanical stability throughout catheter implantation. These excess, thick regions provide surface area on which to apply a fine-tip heat source to shrink the polymer fibers and create a seal without negatively impacting cell viability. The sealed ends of the cylindrical scaffold prevent hMSC migration from either end of the device. In addition, the thick region is utilized throughout catheter delivery, as one thick region is draped over the inner core to absorb the force

exerted on the device as it is plunged through the central fibrous body and inserted into the right ventricle. The utilization of this thick region throughout delivery is shown in Figure 34. The other thick region provides mechanical support as the inner core of the catheter is retracted, inserting the opposite end of the device into the right atrium before the catheter is extracted from the heart. Similar to the both the center thick region and thinner regions previously described, the ends of the scaffold must be at least 40-50 μm thick in order to prevent cell migration through the electrospun pores.

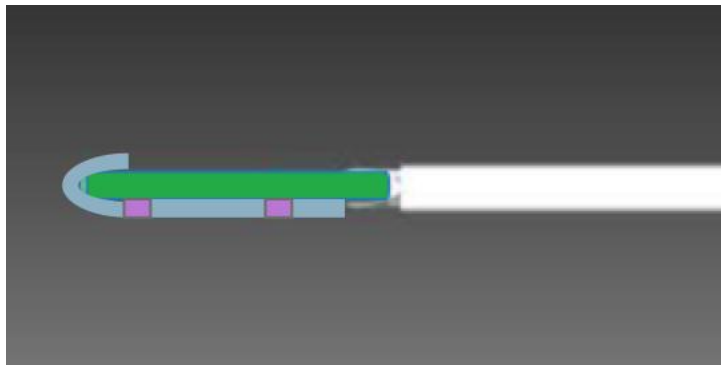


Figure 34: Final design loaded onto specifically designed catheter

To assemble the AV node bypass device, the PU/PET electrospun scaffold consisting of thick and thin regions is manufactured to be a minimum of 2 cm in length and about 1.5-2 mm in outer diameter. About 100,000 hMSCs are then seeded onto a 6x fibrin microthread suture, 2 cm in length and attached to a straight needle. The suture is inserted into one end of the cylindrical scaffold and carefully pulled through. The straight needle is then cut from the suture, leaving the seeded thread within the scaffold. Two pairs of forceps are then used to clamp the edges of the scaffold. A fine-tip heat source set at about 500-600°F is applied to each end until a seal is visually observed. The assembly process of the device is displayed in Figure 35.

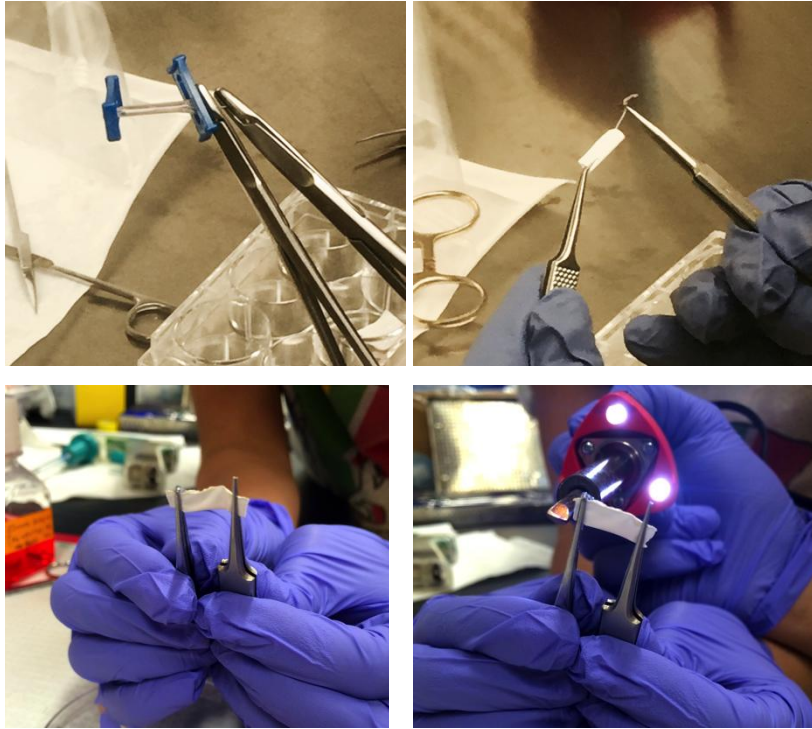


Figure 35: Assembly Method (left to right, top to bottom); a) hMSC seeded fibrin microthread suture is attached to a straight needle b) the suture is inserted and pulled through the cylindrical PU/PET scaffold c) the ends of the scaffold are clamped d) a fine-tip heat source is applied.

Chapter 8: Conclusions and Recommendations

8.1 Future Testing Recommendations

Upon the conclusion of the research project, the team identified a number of recommendations that should be considered in future work to continue the development of the AV node bypass device. The team believes that the completion of these recommended fabrication and testing methods is necessary for the successful advancement of the device to the clinic.

8.1.1 Current Flow

In order to ensure that the heart is properly paced by the AV nodal bypass bridge, voltage stimulation testing should be performed. It is important to ensure that the cells at one end of the bridge are beating at the same rate as the cells at the opposite end of the bridge. This experiment will ensure that the current stimulated at one end of the bridge is successfully collected, carried throughout the bridge and distributed via gap junctions. Cardiomyocytes should be seeded onto two coverslips and kept in a 6 well plate with complete medium. A fibrin microthread seeded with 100,000 hMSCs should be added into the well with one end of the bridge attached to one coverslip, and the other end of the bridge attached to the second coverslip. This attachment will allow for gap junctions to form between the hMSCs and cardiomyocytes. The cardiomyocytes on one of the coverslips should be electrically stimulated at a specific voltage. A reading of the voltage of the second coverslip of cardiomyocytes will be recorded. This reading will be compared with the original voltage to determine the ability of the bridge to pass the current. This experiment should also be performed with a seeded microthread in the

encapsulating scaffold to determine if the overall device is successful in passing the appropriate amount of current.

8.1.2 Mechanical Stability

The mechanical properties of the material will be important, as the scaffold must possess a high degree of elasticity, a high toughness and durability, and a low stiffness to withstand the contractile forces and cyclic loading of the heart. To validate the mechanical integrity of the device, fatigue testing on the Instron machine should be completed. The scaffold should be predisposed to the cyclic loading forces exerted by the heart during contraction.

8.1.3 Gap Junction Formation

To examine the ability of the hMSCs within the bypass device to form gap junctions with the native cardiomyocytes in the heart, immunohistochemistry (IHC) staining for connexin-43 (Cx43) should be performed. Cx43 is a protein embedded in hMSC and cardiomyocyte cell membranes and are responsible for gap junction formation between cells. In accordance with the IHC procedure located in Appendix V, a primary antibody, rabbit-anti-connexin, and a secondary antibody, goat anti-rabbit, should be utilized to tag the Cx43 protein for visualization during fluorescent microscopy imaging. Theoretically, this will lead to images with a high concentration of fluoresced proteins on the edges of adjacent cells. The fluoresced edges will illustrate the presence of connexin 43, and therefore gap junctions between the hMSCs within the bridge and native cardiomyocytes.

This test should initially be performed with fibrin microthreads seeded with 100,000 hMSCs and cardiomyocytes plated in a 12 well plate. Subsequently, this test should be performed on the scaffold samples of different thicknesses. Using the Gaudette-Pins wells, hMSCs should be seeded on one side of the scaffold, while cardiomyocytes should be seeded on

the opposite side. After a pre-determined incubation period, allowing for gap junctions to naturally occur between the two cell types, the scaffold should be stained for Cx43 protein and accompanying gap junctions between the cells. This test will confirm the optimal scaffold thickness needed within the two thinner regions of scaffold, which should all for gap junction formation between hMSCs within the device and native cardiomyocytes.

8.1.4 Physiological Autonomic Responsiveness

To ensure the bypass device offers physiological autonomic responsiveness, catecholamine stimulation testing should be conducted. Each end of the bypass device should be placed within an individual plate of cardiomyocytes and an incubation period should occur. After gap junctions have been allowed to form between the hMSCs within the device and the plated cardiomyocytes, one end of the bypass device should be stimulated using a catecholamine hormone. Epinephrine is one hormone that can be utilized within this procedure, which should increase cellular activity. Theoretically, the effects of the stimulus should be observed initially at the stimulated end of the bridge and then at the second end of the bridge.

8.1.5 Delivery Verification

Testing must be conducted to evaluate and validate the effectiveness of the chosen delivery method, which utilizes a specialized catheter designed by a previous WPI MQP team in 2011. First, the bypass device must be successfully loaded onto the inner core of the catheter device. Following proper loading technique, the catheter delivery should be verified *in vivo* using an animal model. The loaded bypass device should be delivered into a canine heart and the catheter should be extracted via the path of insertion. A cross sectional dissection of the canine heart should be conducted to assess the mechanical integrity of the implanted bypass device throughout insertion. *In vivo* testing using a canine model is necessary to validate successful delivery of the device using the specialized catheter.

8.1.5 Conclusions

The results of the testing verification methods conducted illustrate the progress made in the development of an AV node bypass device utilizing a PU/PET electrospun scaffold and hMSCs. Through the LIVE/DEAD staining of hMSCs on scaffold samples, the PU/PET material was confirmed to be biocompatible. Migration testing results allowed the team to conclude that electrospun scaffold samples of 40 μ m and 50 μ m thickness prevent hMSC migration outside of the bypass device. Scaffold samples of 20 μ m thickness allowed for hMSC migration outside of the insulating scaffold material. An ideal thickness allowing for gap junction formation between hMSCs and native cardiomyocytes should be determined by a future team through the testing of various scaffold thicknesses. This testing will determine the ideal thickness for the thinner regions of the scaffold. The ideal thickness for the thicker regions should also be determined to finalize the device. Finally, the application of a fine-tip heat source at 500°F-600°F successfully seals scaffold ends. The method of heat sealing theoretically prevents cell migration outside of the ends of the device and maintains cell viability.

After speaking to experts in the field, such as Michael Rosen and Ira Cohen, the team believes the presented design for an AV node bypass mechanism is a viable option to treat AV nodal block. Further research and testing on this device will assist in validating the function of the device, eventually bringing the design to the clinic as a replacement for electronic cardiac pacemakers.

References

- [1] Go AS, et. al. Heart Disease and Stroke Statistics—2014 Update: A Report from the American Heart Association. *Circulation*. 2014; 129: e28-e292. Web.
- [2] "Heart Disease Facts." *The Heart Foundation*. n.d. Web. 14 Sept. 2014. Retrieved from <http://www.theheartfoundation.org/heart-disease-facts/heart-disease-statistics/>.
- [3] "What is Heart Block." *National Heart, Lung, and Blood Institute*. 09 July 2012. Web. 18 September 2014. Retrieved from <http://www.nhlbi.nih.gov/health/health-topics/topics/hb/>.
- [4] "What is a Pacemaker?" *National Heart, Lung, and Blood Institute*. 28 February 2012. Web. 18 September 2014. (<http://www.nhlbi.nih.gov/health/health-topics/topics/pace/>).
- [5] "Pacemaker for the Treatment of Heart Failure". *Blue Cross Blue Shield of Tennessee*. n.d. Web. 18 September 2014. (<https://www.bcbst.com/learn/treatment-options/pacemaker.shtm>).
- [6] Cohen IS and Gaudette GR, eds. *Regenerating the Heart: Stem Cells and the Cardiovascular System*. New York: Humana/Springer, 2011; 321-347. Print.
- [7] Chauveau S, Brink PR and Cohen IS. Stem cell–based biological pacemakers from proof of principle to therapy: a review. *Cytotherapy*. 2014; 16(7): 873-880. Web.
- [8] Marieb EN and Hoehn K. *Human Anatomy and Physiology*. Glenview: Pearson Education, Inc. 2013; 9: 659-680. Print.
- [9] Fox SI. *Human Physiology*. New York: The McGraw-Hill Companies, Inc. 2011; 12: 414-419. Print.
- [10] Xin M, Olson EN and Bassell-Duby R. Mending broken hearts: cardiac development as a basis for adult heart regeneration and repair. *Nature Reviews Molecular Cell Biology*. 2013; 14(8): 529-541. Web.
- [11] Sanchez-Quintana D and Ho SY. Anatomy of Cardiac Nodes and Atrioventricular Specialized Conduction System. *Revista Espanola De Cariologia*. 2003; 56(11): 1085-1092. Web.
- [12] Kurian T, Ambrosi C, Hucker W, Fedorov VV and Efimov IR. Anatomy and Electrophysiology of the Human AV Node. *Pacing and Clinical Electrophysiology*. 2010; 33(6): 754-762. Web.

- [13] James TN and Sherf L. Ultrastructure of the Human Atrioventricular Node. *Circulation*. 1968; 37: 1049-1070. Web.
- [14] Temple IP, Inada S, Dobrzynski H and Boyett MR. Connexins and the atrioventricular node. *Heart Rhythm*. 2013; 10(2): 297-304. Web.
- [15] Goldreyer BN and Damato AN. The Essential Role of Atrioventricular Conduction Delay in the Initiation of Paroxysmal Supraventricular Tachycardia. *Circulation*. 1971; 43: 679-687. Web.
- [16] Accili EA, Proenza C, Baruscotti M and DiFrancesco D. From Funny Current to HCN Channels: 20 Years of Excitation. *Physiology*. 2002; 17(1): 32-37. Web.
- [17] Camelliti, P. Fibroblast Network in Rabbit Sinoatrial Node: Structural and Functional Identification of Homogeneous and Heterogeneous Cell Coupling. *Circulation Research*. 2004; 94(6): 828-35. Web.
- [18] Shih, H. Anatomy of the Action Potential in the Heart. *Molecular and Cellular Cardiology*. 1994; 21(1): 30-41. Web.
- [19] Biel M, Schneider A and Wahl C. Cardiac HCN channels: Structure, function, and modulation. *Trends Cardiovasc Med*. 2002; 12: 206-212. Web.
- [20] Gregoratos G, Cheitlin M, Conill A, Epstein A, Fellows C, Ferguson T, Freedman R, Hlatky M, Naccarelli G, Saksena S, Schlant R and Silka M. ACC/AHA Guidelines for Implantation of Cardiac Pacemakers and Antiarrhythmia Devices: Executive Summary - a report of the American College of Cardiology/American Heart Association Task Force on Practice Guidelines (Committee on Pacemaker Implantation). *Circulation*. 1998; 97: 1325-35. Web.
- [21] Simson MB. Use of signals in the terminal QRS complex to identify patients with ventricular tachycardia after myocardial infarction. *Circulation*. 1981; 64: 235-242.
- [22] Scholten A. Bradycardia. *EBSCO Publishing*. 2011; 1-4. Web.
- [23] Mann DL, Zipes DP, Libby P and Bonow RO. Braunwald's Heart Disease: A Textbook of Cardiovascular Medicine. *Elsevier Health Sciences*. 2014; 796.
- [24] Greenspon AJ, Patel JD, Lau E, Ochoa JA, Frisch DR, Ho RT, Pavri BB, and Kurtz SM. Trends in Permanent Pacemaker Implantation in the United States From 1993 to 2009: Increasing Complexity of Patients and Procedures. *Journal of the American College of Cardiology*. 2012; 60(16): 1540-1545. Web.
- [25] Ottenberg AL, Mueller LA, Mueller PS. Perspectives of patients with cardiovascular implantable electronic devices who received advisory warnings. *Heart & Lung: The Journal of Acute and Critical Care*. 2013; 42(1): 59-64. Web.

- [26] Marieb EN and Hoehn K. *Human Anatomy and Physiology*. Glenview: Pearson Education, Inc. 2013; 9: 684. Print.
- [27] Marieb EN and Hoehn K. *Human Anatomy and Physiology*. Glenview: Pearson Education, Inc. 2013; 9: 414-416. Print.
- [28] Durrani S, Konoplyannikov M, Ashraf M and Haider KH. Skeletal myoblasts for cardiac repair. *Regen Med*. 2010; 5: 919–932. Web.
- [29] Kehat I, Khimovich L, Caspi O, Gepstein A, Shofti R, Arbel G, Huber I, Satin J, Itskovitz-Eldor J and Gepstein L. Electromechanical integration of cardiomyocytes derived from human embryonic stem cells. *Nat Biotechnology*. 2004; 22: 1282-1289. Web.
- [30] Ma J, Guo L, Fiene SJ, Anson BD, Thomson JA, Kamp TJ, Kolaja KL and Swanson BJ. High purity human-induced pluripotent stem cell-derived cardiomyocytes: Electrophysiological properties of action potentials and ionic currents. *Am J Physiol Heart Circ Physiol*. 2006; 301: 2017. Web.
- [31] Yao J, Morioka T and Oite T. PDGF regulates gap junction communication and connexin 43 phosphorylation by PI 3-kinase in mesangial cells. *Kidney International*. 2000; 57: 1915–1926. Web.
- [32] Jung S, Panchalingam K, Rosenberg L and Behie L. Ex Vivo Expansion of Human Mesenchymal Stem Cells in Defined Serum-Free Media. *Stem Cells International*. 2012; 1-21. Web.
- [33] Hare JM, Traverse JH, Henry TD, Dib N, Strumpf RK, Schulman SP, Gerstenblith G, DeMaria AN, Denktas AE, Gammon RS, Hermiller JB, Jr., Reisman MA, Schaer GL and Sherman W. A randomized, double-blind, placebo-controlled, dose-escalation study of intravenous adult human mesenchymal stem cells (prochymal) after acute myocardial infarction. *J Am Coll Cardiol*. 2009; 54: 2277-2286. Web.
- [34] Yanagi K, Takano M, Narazaki G, Uosaki H, Hoshino T, Ishii T, Misaki T, and Yamashita JK. Hyperpolarization-Activated Cyclic Nucleotide-Gated Channels and T-Type Calcium Channels Confer Automaticity of Embryonic Stem Cell-Derived Cardiomyocytes. *Stem Cells*. 2007; 25(11): 2712-2719. Web.
- [35] Valiunas, V. Human Mesenchymal Stem Cells Make Cardiac Connexins and Form Functional Gap Junctions. *The Journal of Physiology*. 2004; 555(3): 617-26. Web.
- [36] Pittenger MF and Martin BJ. Mesenchymal stem cells and their potential as cardiac therapeutics. *Circ Res*. 2004; 95: 9-20. Web.
- [37] Plotnikov AN, Shlapakova I, Szabolcs MJ, Danilo P, Jr., Lorell BH, Potapova IA, Lu Z, Rosen AB, Mathias RT, Brink PR, Robinson RB, Cohen IS and Rosen MR. Xenografted

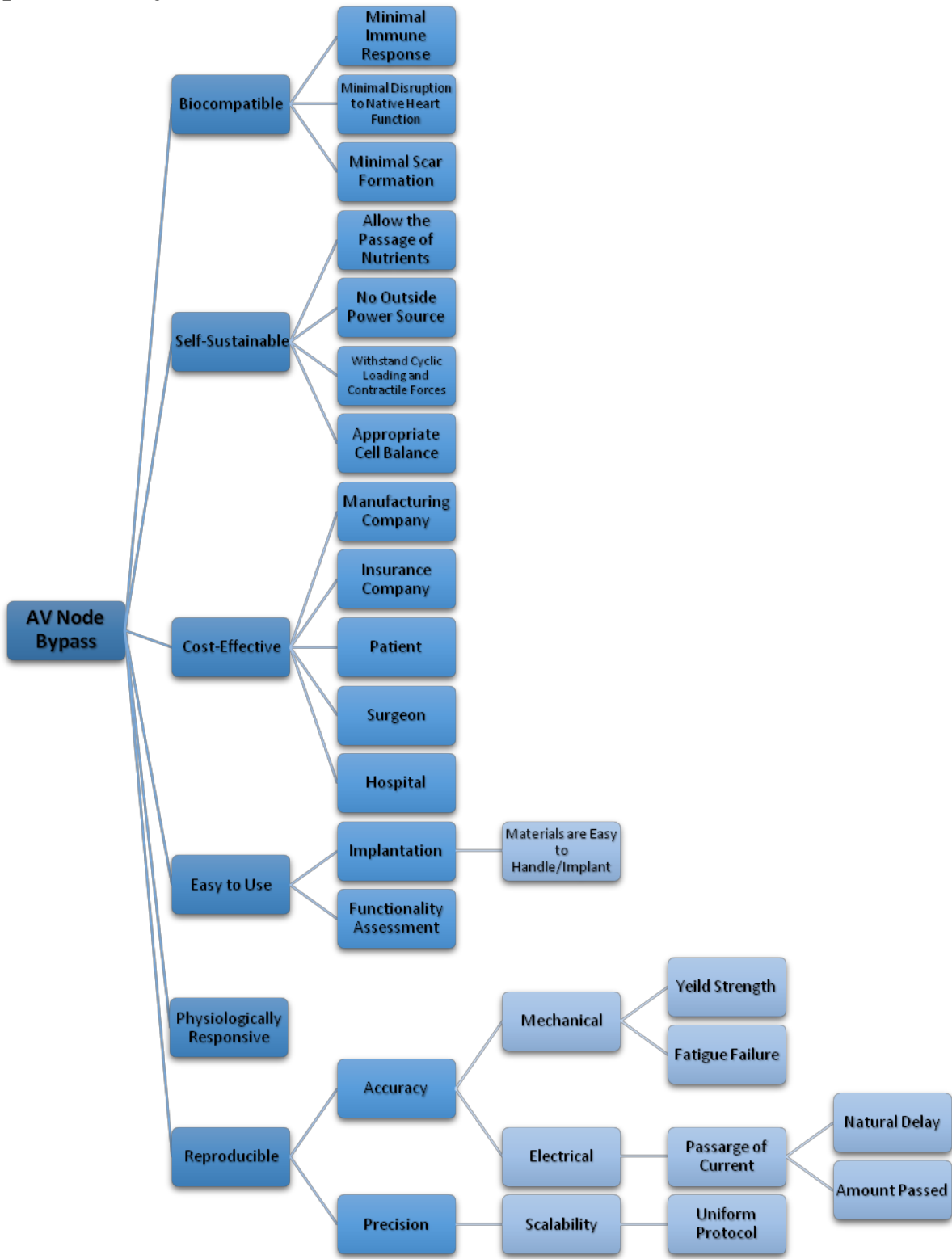
- adult human mesenchymal stem cells provide a platform for sustained biological pacemaker function in canine heart. *Circulation*. 2007; 116: 706-713. Web.
- [38] Qu, J. Expression and Function of a Biological Pacemaker in Canine Heart. *Circulation*. 2003; 107(8): 1106-109. Web.
- [39] Cho HC, Kashiwakura Y and Marban E. Creation of a biological pacemaker by cell fusion. *Circ Res*. 2007; 100: 1112-1115. Web.
- [40] Rosen AB, Kelly DJ, Schuldt AJT, Lu J, Potapova IA, Doronin SV, Robichaud KJ, Robinson RB, Rosen MR, Brink PR, Gaudette GR and Cohen IS. Finding Fluorescent Needles in the Cardiac Haystack: Tracking Human Mesenchymal Stem Cells Labeled with Quantum Dots for Quantitative In Vivo Three-Dimensional Fluorescence Analysis. *STEM CELLS*. 2007; 25: 2128–2138. Web.
- [41] Cornwell K, and Pins G. Discrete crosslinked fibrin microthread scaffolds for tissue regeneration. *Journal of Biomedical Materials Research: Part A*. 2007; 82: 104-112. Web.
- [42] Cornwell K. Collagen and fibrin biopolymer microthreads for bioengineered ligament generation: A dissertation. *University of Massachusetts Medical School. Graduate School of Biomedical Sciences*. 2007. Web.
- [43] Christman K, et al. Injectable fibrin scaffold improves cell transplant survival, reduces infarct expansion, and induces neovasculature formation in ischemic myocardium. *J Am Coll Cardiol*. 2004; 44(3): 654-60. Web.
- [44] Wendt D, Marsano A, Jakob M, Heberer M and Martin I. Oscillating perfusion of cell suspensions through three-dimensional scaffolds enhances cell seeding efficiency and uniformity. *Biotechnol Bioeng*. 2003; 84(2): 205-214. Web.
- [45] Grasman JM, Page RL, Dominko T and Pins GD. Crosslinking strategies facilitate tunable structural properties of fibrin microthreads. *Acta Biomaterialia*. 2012; 8(11): 4020-4030. Web.
- [46] Guyette JP, Fakharzadeh M, Burford EJ, Tao ZW, Pins GD, Rolle MW, Gaudette GR. A novel suture-based method for efficient transplantation of stem cells. *Journal of Biomedical Materials Research*. 2013; 101A: 809-818.
- [47] Page RL, Malcuit C, Vilner L, Vojtic I, Shaw S, Hedblom E, Hu J, Pins G, Rolle M and Dominko T. Restoration of Skeletal Muscle Defects with Adult Human Cells Delivered on Fibrin Microthreads. *Mary Ann Liebert, Inc*. 2011; 17. Web.
- [48] DiTroia L, Hassett H and Roberts J. Fibrin microthreads for stem cell delivery in cardiac applications. *Worcester Polytechnic Institute: Major Qualifying Project*. 2008. Web.

- [49] Drexler H, Meyer G and Wollert K. Bone-marrow-derived cell transfer after ST-elevation myocardial infarction: lessons from the BOOST trial. *Nat Clin Pract Cardiovasc Med*. 2006; 3 (Suppl. 1): S65-S68. Web.
- [50] Wung N, Acott SM, Tosh D and Ellis MJ. Hollow fibre membrane bioreactors for tissue engineering applications. *Biotechnol Lett*. 2014; 36: 2357-2366. Web.
- [51] Wendorff JH, et al. *Electrospinning: Materials, Processing and Applications*. Hoboken: John Wiley & Sons. 2012. 16-18. Web.
- [52] Khil MS, et al. Electrospun nanofibrous polyurethane membrane as wound dressing. *Journal of Biomedical Materials Research Part B: Applied Biomaterials*. 2003. 67B(2). 675-679. Web.
- [53] Pedicini A, et al. Mechanical behavior of electrospun polyurethane. *Polymer*. 2003. 44(22). 6857-6862. Web.
- [54] Bioglue ® Surgical Adhesive. *CryoLife*. 2015. Web. 2 March 2015. Retrieved from: <http://www.cryolife.com/products/bioglue-surgical-adhesive>
- [55] Heat Sealers. Stapler Warehouse. 2013. Web. 2 March 2015. Retrieved from: <http://www.staplerwarehouse.com/c-51-heat-sealers.aspx>
- [56] Sherman W, Martens TP, Viles-Gonzalez JF and Siminiak T. Catheter-based Delivery of Cells to the Heart. *Nature Clinical Practice Cardiovascular Medicine*. 2006; 3(3): S57-64.
- [57] Costa EJ, Hanna BE, Madden AT and Olsen TM. A Cardiac Catheterization Device for the Delivery of Human Mesenchymal Stem Cells. *Worcester Polytechnic Institute: Major Qualifying Project*. 2011. Web.
- [58] Alfonzo H, Ali S, Almeida B and Flynn K. Cardiac Scaffold for Human Mesenchymal Stem Cell Facilitated Autonomous Pacing. *Worcester Polytechnic Institute: Major Qualifying Project*. 2009. Web.
- [59] Tatai L, Moore TG, Adhikari R, Malherbe F, Jayasekara R, Griffiths I and Gunatillake PA. Thermoplastic biodegradable polyurethanes: The effect of chain extender structure on properties and in-vitro degradation. *Biomaterials*. 2007; 28(36): 5407-5417. Web.
- [60] Ates B, Koytepe S, Karaaslan MG, Balcioglu S and Gulgen S. Biodegradable non-aromatic adhesive polyurethanes based on disaccharides for medical applications. *International Journal of Adhesion and Adhesives*. 2014; 49: 90-96. Web.
- [61] Kanyanta V and Ivankovic A. Mechanical characterisation of polyurethane elastomer for biomedical applications. *Journal of the Mechanical Behavior of Biomedical Materials*. 2010; 3(1): 51-62. Web.

- [62] Polyurethanes and Thermal Degradation Guidance. American Chemistry Council's Center for the Polyurethanes Industry. March 2014. Web. 2 March 2015.
(<http://polyurethane.americanchemistry.com/Resources-and-Document-Library/6936.pdf>)
- [63] Limam M, Tighzert L, Fricoteaux F and Bureau G. Sorption of organic solvents by packaging materials: polyethylene terephthalate and TOPAS®. *Polymer Testing*. 2005; 24(3): 395-402. Web.
- [64] Rae PJ and Dattelbaum DM. The properties of poly(tetrafluoroethylene) (PTFE) in compression. *Polymer*. 2004; 45(22): 7615-7625. Web.
- [65] Mehta RI, Mukherjee AK, Patterson TD and Fishbein MC. Pathology of explanted polytetrafluoroethylene vascular grafts. *Cardiovascular Pathology*. 2011; 20(4): 213-221. Web.
- [66] Alfonso, H, Ali, S, Almeida, B, Flynn, K. Cardiac Scaffold for Human Mesenchymal Stem Cell Facilitated Autonomous Pacing. *Worcester Polytechnic Institute: Major Qualifying Project*. 2009. Web.
- [67] Chunis, P, Qiao, J, Sood, D, Whitman, M. Implantable Biological Pacemaker for Permanent Autonomous Pacing of the Heart. *Worcester Polytechnic Institute: Major Qualifying Project*. 2012. Web.
- [68] Gaudette G, Phaneuf MD, Ali S, Almeida B, Alfonso H and Flynn K. Nanofiber scaffold (Patent Number: US 20110142804 A1). *Google Patents*. 2010. Web.

Appendices

Appendix I: Objectives Tree



Appendix II: Pairwise Comparison Charts

Primary PCC:

	Biocompatible	Physiologically Responsive	Self-Sustaining	Cost-Effective	Easy to Use	Reproducible	Deliverable	Total
Biocompatible								
Physiologically Responsive								
Self-Sustaining								
Cost-Effective								
Easy to Use								
Reproducible								
Deliverable								

Secondary PCCs:

Biocompatible	Immune Response	Disruption	Scar Formation	Total
Immune Response				
Disruption to Contractile System				
Scar Formation				

Self-Sustaining	Nutrients	Power Source	Cell Balance	Withstand	Total
Nutrients					
Power Source					
Cell Balance					
Withstand Loading & Forces					

Cost-Effective	Manufacturing	Insurance	Patient	Surgeon	Hospital	Total
Manufacturing						
Insurance						
Patient						
Surgeon						
Hospital						

Reproducible - Accuracy	Mechanical	Electrical	Biological	Total
Mechanical				
Electrical				
Biological				

Deliverable	Compatible	Minimally Invasive	Implantable	Total
Compatible				
Minimally Invasive				
Implantable				

Appendix III: LIVE/DEAD Staining Protocol

Preparation for staining on scaffold:

1. Cut scaffold samples and place into a well plate
2. Sterilize scaffold samples in the well plate via ethylene oxide treatment
3. After de-gassing period, add complete medium to the wells with scaffolds
4. Seed scaffold samples with approximately 40,000 hMSCs by pipetting cell suspension directly onto the scaffolds
5. Seed 40,000 hMSCs into one of the wells in the well plate to be a dead control
6. Incubate samples for 1 and 4 days
7. Follow procedure below after 1 and 4 days

Reagents:

Solution 1:

1. 1.0mL Serum Free DMEM
2. 1.0 μ L Ethidium Homodimer-1
3. 1.0 μ L Calcein AM

Solution 2:

1. 1.0mL Serum Free DMEM
2. 1.0 μ L Ethidium Homodimer-1
3. 1.0 μ L Calcein AM
4. 0.5 μ L Hoechst Dye

Procedure:

1. Incubate dead controls in 70% Ethanol for 30 minutes prior to experiment
2. Mix solution 1 within 1 hour of use
3. Incubate cells with solution 1 for 15 minutes
4. Mix solution 2 within 1 hour of use
5. Incubate cells in solution 2 for 15 minutes
6. Wash cells with 1x PBS 3 times
7. Fix cells in 4% Phosphate buffered formaldehyde for 10 minutes
8. Mount scaffold on coverslip and image

Appendix IV: Hoechst and Phalloidin Staining Protocol

Preparation for Scaffold Staining:

1. Cut scaffold samples to the size of the Gaudette-Pins well
2. Sterilize the sample/well with ethylene oxide treatment
3. Place Gaudette-Pins with scaffold onto 6 well plate with complete media
4. Seed scaffold sample in the Gaudette-Pins well with 80,000 hMSCs by pipetting cell suspension directly onto the scaffold
5. Incubate samples for (at least) 4 days
6. Follow Procedure below

Reagents:

1. DPBS
2. 4% paraformaldehyde
3. 0.25% Triton-X
4. 1% BSA
5. Phalloidin
6. Hoechst

Procedure:

1. Aspirate media
2. Rinse with DPBS x2
3. Fix in 4% paraformaldehyde for 10 minutes
4. Rinse with DPBS x2
5. Remove scaffold from Gaudette/Pins well and place in 6 well plate
6. Block with BSA solution for 30 minutes
7. Phalloidin solution for 30 minutes
8. Rinse with DPBS x2
9. Hoechst solution for 3-5 minutes
10. Rinse with DPBS x2
11. Mount scaffold on coverslip and image

Appendix V: Immunohistochemistry Cx43 Staining Protocol

Preparation for IHC Staining:

1. Obtain 6x thread bundle (or a variation of bundle)
2. Cut into 2-3 cm sutures
3. Quantum Dot Load 100,000 hMSCs
4. Seed with 100,000 hMSCs on for 24 hours
5. Incubate seeded threads for a minimum of 48 hours in complete media
6. Aspirate media and remove seeded thread from tissue culture plate
7. Place seeded thread into 6, 12 or 24 well plate containing neonatal rat cardiomyocytes
8. Incubate for an appropriate period of time
9. Seed an appropriate amount of hMSCs onto a separate tissue culture dish/well containing neonatal rat cardiomyocytes. Incubate for an appropriate period of time
10. Follow Staining Procedure Below

Reagents:

1. Cold acetone
2. 5% Normal Goat (or Rabbit) Serum in PBS
3. Primary antibody: mouse anti-connexin (or anti-alpha actinin) 1:100 in 5% NGS (or NRS)
4. Secondary antibody: goat (or rabbit) anti-mouse Alexa Fluor 546 1:400 in 5% NGS (or NRS)
5. Hoechst stain:
 - a. 0.0167% Hoechst dye in PBS
 - b. 0.5 μ L in 3000 μ L PBS
6. 0.25% Triton X-100
7. Phalloidin (AF 488 Phalloidin)

Procedure:

1. Fix cells with paraformaldehyde for 10 minutes at room temperature
2. 3 washes in PBS (5 minutes each)
3. Place samples in cold acetone - place in freezer at -20 degrees Celcius for 10 minutes
4. 3 washes in PBS (5 minutes each)
5. 0.25% Triton X-100 – 10 minutes
6. Block with 5% Normal Goat (or rabbit) Serum for 45 minutes
 - a. 400microliters of 100% goat serum in 8mL of PBS
7. Leave goat (or rabbit) serum on negative sample, aspirate off the positive sample
8. Primary mouse anti-connexin (and/or anti-alphaactinin) added only to positive sample in cold room - leave overnight in refrigerator
 - a. 2microliters primary in 200microliters PBS
9. 3 washes in PBS (5 minutes each)
10. Secondary goat (or rabbit) anti-mouse Alexa Fluor 546 AND the phalloidin solution added to both samples, left for 1 hour in the dark
11. 3 washes in PBS (5 minutes each with lid closed)

12. Hoechst stain - 0.5microliters Hoechst in 3000microliters PBS (left for 5 minutes with lid closed)
13. 3 washes in PBS (5 minutes each with lid closed)
14. Put coverslip on tissue sample slide
 - a. Get water off, drop cyto seal, make sure no air bubbles
15. Image